

A unified statistical model for S-N fatigue curves: probabilistic definition

*Original*

A unified statistical model for S-N fatigue curves: probabilistic definition / Paolino, Davide Salvatore; Chiandussi, Giorgio; Rossetto, Massimo. - In: FATIGUE & FRACTURE OF ENGINEERING MATERIALS & STRUCTURES. - ISSN 8756-758X. - STAMPA. - 36:3(2013), pp. 187-201. [10.1111/j.1460-2695.2012.01711.x]

*Availability:*

This version is available at: 11583/2497435 since:

*Publisher:*

Wiley-Blackwell

*Published*

DOI:10.1111/j.1460-2695.2012.01711.x

*Terms of use:*

This article is made available under terms and conditions as specified in the corresponding bibliographic description in the repository

*Publisher copyright*

(Article begins on next page)

**Please cite this article as:**

“PAOLINO, D.S., CHIANDUSSI, G. and ROSSETTO, M., 2013. A unified statistical model for S-N fatigue curves: Probabilistic definition. *Fatigue and Fracture of Engineering Materials and Structures*, **36**(3), pp. 187-201.”

# A unified statistical model for S-N fatigue curves: probabilistic definition

## Authors:

D.S. Paolino<sup>a</sup>, G. Chiandussi<sup>b</sup>, M. Rossetto<sup>c</sup>

<sup>a</sup> Department of Mechanical and Aerospace Engineering, Politecnico di Torino, 10129 Turin, Italy,  
davide.paolino@polito.it

<sup>b</sup> Department of Mechanical and Aerospace Engineering, Politecnico di Torino, 10129 Turin, Italy,  
giorgio.chiandussi@polito.it

<sup>c</sup> Department of Mechanical and Aerospace Engineering, Politecnico di Torino, 10129 Turin, Italy,  
massimo.rossetto@polito.it

## Corresponding Author:

D.S. Paolino

*E-mail address:* davide.paolino@polito.it

*Full postal address:*

C.so Duca degli Abruzzi 24,

Department of Mechanical and Aerospace Engineering – Politecnico di Torino,

10129 – Turin,

ITALY

*Phone number:* +39.011.090.5746

*Fax number:* +39.011.090.6999

**Abstract:**

In recent years, experimental tests exploring the gigacycle fatigue properties of materials suggest the introduction of modifications in well known statistical fatigue life models. Usual fatigue life models, characterized by a single failure mechanism and by the presence of the fatigue limit, have been integrated by models that can take into account the occurrence of two failure mechanisms and do not consider the presence of the fatigue limit. The general case, in which more than two failure mechanisms coexist with the fatigue limit, has not been proposed yet.

The paper presents a unified statistical model which can take into account any number of failure mechanisms and the possible presence of the fatigue limit. The case of S-N curves with different fatigue life distributions coexisting for the entire stress range covered by fatigue tests is also considered. The adaptability of the statistical model to the S-N curves proposed in the open literature is demonstrated by qualitative numerical examples.

**Keywords:**

Gigacycle fatigue; Failure modes; Random fatigue limit; Random fatigue life

## Nomenclature

$c_i$  = number of failure causes generating the  $i$ -th failure mode

$C_1, \dots, C_i, \dots, C_m$  = random variables representing failure causes

$F_{X_l}, F_{X_t}, F_{X_{t_0}}, F_{X_{t_m}}, F_Y, F_{Y|int}, F_{Y|surf}$  = cumulative distribution functions

$int$  = internal-initiated failure

$m$  = number of failure modes

$M$  = random variable representing failure mode

$n_{par}$  = total number of parameters

$P[\cdot]$  = probability of an event

$p_{j|i}$  = probability of having the  $j$ -th failure cause within the  $i$ -th failure mode

$q_{i,rand}$  =  $i$ -th random probability value

$surf$  = surface-initiated failure

$x$  = stress amplitude value

$X_l$  = random variable representing fatigue limit

$x_{l,max}$  = upper limit value of  $X_l$

$X_t, X_{t_0}, X_{t_1}, X_{t_2}, \dots, X_{t_{m-1}}, X_{t_m}$  = random variable representing transition stresses

$x_{t,min}$  = lower limit value of  $X_t$

$y$  = fatigue life value

$y_{i,rand}$  =  $i$ -th random fatigue life value

$Y$  = random variable representing fatigue life

$Y|(i, j)$  = conditional random variable representing fatigue life given that  $M = i$  and  $C_i = j$

$Y|int$  = conditional random variable representing fatigue life given that  $M = int$

$Y|surf$  = conditional random variable representing fatigue life given that  $M = surf$

$\Phi[\cdot]$  = standardized Normal cumulative distribution function

$\mu_{X_l}, \mu_{X_t}, \mu_{X_{t_{i-1}}}, \mu_{Y|(i,j)}, \mu_{Y|int}, \mu_{Y|surf}$  = location parameters

$a_{Y|(i,j)}, b_{Y|(i,j)}$  = parameters involved in  $\mu_{Y|(i,j)}$

$a_{Y|int}, b_{Y|int}$  = parameters involved in  $\mu_{Y|int}$

$a_{Y|surf}, b_{Y|surf}$  = parameters involved in  $\mu_{Y|surf}$

$\sigma_{X_l}, \sigma_{X_t}, \sigma_{X_{t_{i-1}}}, \sigma_{Y|(i,j)}, \sigma_{Y|int}, \sigma_{Y|surf}$  = scale parameters

$\cdot | \cdot$  = conditional event

## 1. Introduction

In recent years, experimental tests exploring the gigacycle fatigue properties of materials suggest the introduction of modifications in well known statistical fatigue life models<sup>1</sup>.

In some cases<sup>2-6</sup>, it has been found that specimens may fail even if the applied stress value is smaller than the usual (conventional) fatigue limit. In most cases, while interior-initiated failures occur if the applied stress amplitude is smaller than the usual fatigue limit, failures due to crack nucleation at surface defects occur when the applied stress amplitude is larger than the usual fatigue limit. Therefore two distinct failure mechanisms are visible in fatigue data plots and, at a stress value near the usual fatigue limit, plots show a plateau separating the two failure mechanisms. For this reason, the usual fatigue limit can be considered as a transition stress that differentiates between two failure mechanisms. More generally, plateaux separating different failure mechanisms represent transition stresses, while plateaux separating finite lives from infinite lives can be considered as a real fatigue limit, if it exists<sup>1,7</sup>.

Moreover, recent studies<sup>5,8-12</sup> have found that different fatigue life distributions may coexist. The presence of different fatigue life distributions in data plots can be explained by assuming that distinct mechanisms of failure may coexist for a wide range of the applied stress amplitude. Indeed, fractographs<sup>5,10</sup> have shown that inclusions with different properties<sup>13</sup> may lead to interior-initiated failures at different average fatigue lives and, as a consequence, can be considered as different mechanisms of failure. Jha et al.<sup>8</sup> mentioned that different sizes of  $\alpha_2$  colonies in a  $\gamma$ -TiAl based alloy may be the cause of different fatigue lives. Finally, in<sup>8,9,11,12</sup> the presence of different life distributions in the same stress range is explained by considering the environmental effect: for some materials, a quasi-vacuum environment may significantly delay crack nucleation.

In the following, according to what suggested by Harlow<sup>14</sup>, if failure mechanisms are separated by plateaux, then they are called failure modes; while, if failure mechanisms coexist for the same range of the applied stress amplitude and, consequently, are not distinguished by plateaux, then they are called failure causes.

To the authors' best knowledge, a unified statistical model able to describe any S-N curve regardless of the number of failure modes and failure causes has not been identified yet. Usually, specific statistical fatigue models are used in order to fit specific experimental data. In many international standards<sup>15,16</sup> statistical fatigue models, able to describe experimental data with one failure mode due to one failure cause, are obtained by taking into account a linear function for the mean fatigue life and by considering a constant standard deviation for the fatigue life. By considering different probabilistic approaches (e.g., the random fatigue-limit model<sup>17,18</sup>, the weakest-link principle<sup>19</sup>, the equivalent fatigue strength concept<sup>20</sup>), the capability of taking into account the presence of the fatigue limit has been added in some statistical fatigue models. Recently<sup>21-23</sup>, a series system approach for competing failure modes<sup>24,25</sup> has been adopted for experimental data with two different failure causes. While, for the same type of experimental data, some other researchers<sup>6,8,26</sup> proposed an approach based on a mixture of distributions<sup>24,27</sup>.

A unified statistical model able to describe any S-N curve regardless of the number of failure modes and failure causes is obtained in the following. The adaptability of the proposed model is demonstrated by qualitative numerical examples.

## 2. Duplex S-N curve

Figure 1 shows a typical gigacycle fatigue data plot with two plateaux: the upper plateau represents a transition stress, while the lower plateau represents a fatigue limit. This kind of plot is defined as duplex S-N curve<sup>6</sup>.

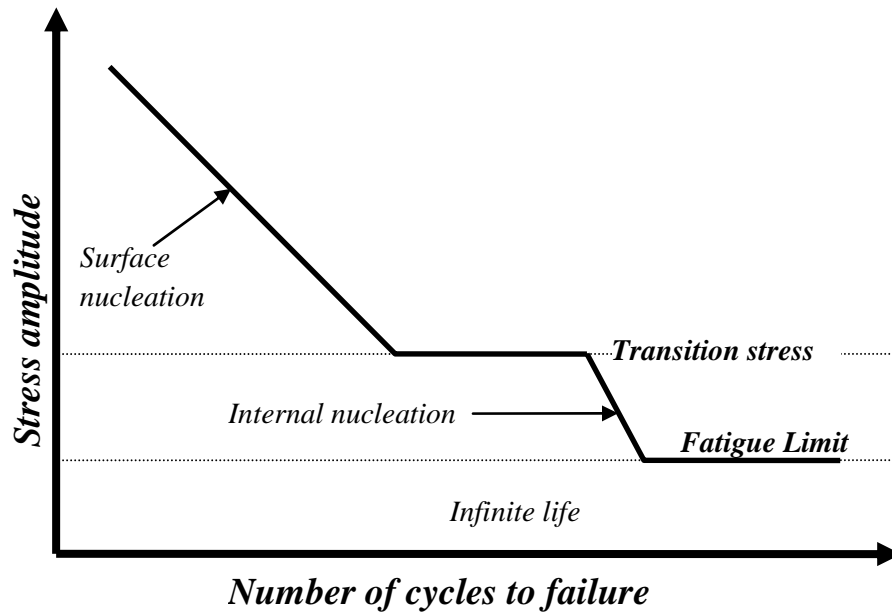


Figure 1: Typical duplex S-N curve.

The statistical fatigue life model for duplex S-N curves and its defining parameters are described in the following sections.

### 2.1 Duplex S-N curve: statistical fatigue life model

Some initial hypotheses are required in order to identify a statistical fatigue life model for duplex S-N curves:

- 1) the fatigue limit,  $X_l$ , is a random variable (rv) with cumulative distribution function (cdf)  $F_{X_l}$ : fatigue limit values vary randomly from specimen to specimen, even if specimens are made of the same nominal material;
- 2) the transition stress,  $X_t$ , is a rv with cdf  $F_{X_t}$ : transition stress values vary randomly from specimen to specimen, even if specimens are made of the same nominal material;
- 3)  $X_l$  and  $X_t$  are independent rv's;
- 4) the failure mode,  $M$ , is a Bernoulli rv with realizations: internal-initiated failure,  $int$ , and surface-initiated failure,  $surf$ ;
- 5) the fatigue life given that  $M = int$  is a conditional rv,  $Y|int$ , with cdf  $F_{Y|int}$ ;
- 6) the fatigue life given that  $M = surf$  is a conditional rv,  $Y|surf$ , with cdf  $F_{Y|surf}$ ;

By considering hypotheses 1)-4), the probability of having a surface-initiated failure is as follows:

$$P[M = surf] = F_{X_l}F_{X_t}, \quad (1)$$

while the probability of having an interior-initiated failure is given by:

$$P[M = int] = F_{X_l}(1 - F_{X_t}). \quad (2)$$

In particular, Equation (1) can be derived by considering that the probability of having a surface-initiated failure is equal to the probability that both  $X_l$  and  $X_t$  are smaller than a given stress amplitude value,  $x$ . While Equation (2) can be obtained by considering that the probability of having an interior-initiated failure is equal to the probability that  $x$  is between  $X_l$  and  $X_t$ .

It must be pointed out that, if  $X_l$  and  $X_t$  are continuous rv's defined on the whole stress amplitude axis, there is a nonzero probability of having a specimen with the fatigue limit larger than the transition stress. This is not acceptable from a physical point of view, since it would mean that interior-initiated failures could occur even if the applied stress amplitude is smaller than the fatigue limit of the specimen. Thus, a seventh hypothesis must be added:

7) the event  $X_l \leq X_t$  is almost sure (i.e.,  $P[X_l \leq X_t] = 1$ ).

It is worth noting that hypothesis 7) adds a constraint to the relationship between the distributions of  $X_l$  and  $X_t$  but it is not in contrast with hypothesis 3). Indeed, in order to fulfill hypothesis 7) it is sufficient to assume for  $X_l$  a continuous distribution with a fixed upper limit value, say  $x_{l,max}$ , and for  $X_t$  a continuous distribution with a fixed lower limit value, say  $x_{t,min}$ , larger than  $x_{l,max}$ . Once defined the range of validity of the two distributions, random values for  $X_l$  and  $X_t$  can be independently drawn, thus fulfilling hypothesis 3).

As shown in Figure 2, hypothesis 7) can be graphically visualized with a stress amplitude axis representation concerning a single specimen.

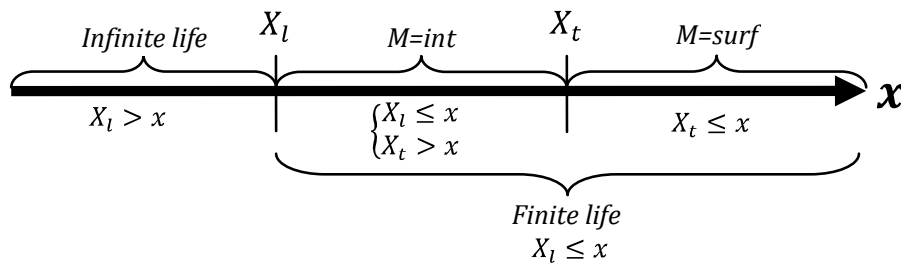


**Figure 2:** Stress amplitude axis representation of hypothesis 7); duplex S-N curve.

According to hypotheses 3) and 7) and with reference to Figure 2, Equation (1) can be further simplified as follows:

$$P[M = surf] = P[X_t \leq x] = F_{X_t}. \quad (3)$$

It is worth noting that, as explained by Cox<sup>24</sup>, two failure modes can be considered as mutually exclusive if a “single risk” model applies: i.e., if specimens belong to two different populations and



a specimen of the first (second) population may fail only for the first (second) failure mode. Indeed, a “single risk” model can be adopted in this case, since it can be statistically shown<sup>9,28</sup> that surface-initiated failures (first failure mode) occur only when specimens have at least one surface defect (first population), while interior-initiated failures (second failure mode) occur only when specimens present no surface defect at all (second population).

By taking into account hypotheses 4)-6), the probability of having a surface-initiated failure with fatigue life,  $Y$ , smaller than a specific fatigue life value,  $y$ , is given by:

$$P[Y \leq y, M = surf] = P[Y \leq y | M = surf] \cdot P[M = surf] = F_{Y|surf} F_{X_t}, \quad (4)$$

while the probability of having an interior-initiated failure with  $Y$  smaller than  $y$  is given by:

$$P[Y \leq y, M = int] = P[Y \leq y | M = int] \cdot P[M = int] = F_{Y|int} F_{X_l} (1 - F_{X_t}). \quad (5)$$

As shown in Figure 2, the events  $M = surf$  and  $M = int$  form a partition of the set of finite lives; therefore, as an easy application of the Total Probability Theorem, it follows that the cdf of  $Y$  is finally given by:

$$F_Y = F_{Y|surf} F_{X_t} + F_{Y|int} F_{X_l} (1 - F_{X_t}), \quad (6)$$

which represents the statistical fatigue life model for duplex S-N curves.

## 2.2. Duplex S-N curve: parameters

The cdf  $F_Y$  given in (6) depends on the cdf's of the continuous rv's  $X_l$ ,  $X_t$ ,  $Y|int$  and  $Y|surf$ . According to what proposed in the literature<sup>17,18,20,29</sup> for the fatigue strength, both  $X_l$  and  $X_t$  can be considered location-scale (e.g., Normal) or log-location-scale (e.g., Weibull of Log-Normal) rv's. Without loss of generality, in the following both  $X_l$  and  $X_t$  are supposed to be Normal distributed. In particular, let  $X_l$  have location parameter  $\mu_{X_l}$  and scale parameter  $\sigma_{X_l}$ , and  $X_t$  have location parameter  $\mu_{X_t}$  and scale parameter  $\sigma_{X_t}$ , then:

$$F_{X_l} = \Phi \left[ \frac{x - \mu_{X_l}}{\sigma_{X_l}} \right], \quad (7)$$

and

$$F_{X_t} = \Phi \left[ \frac{x - \mu_{X_t}}{\sigma_{X_t}} \right], \quad (8)$$

where  $\Phi$  is the standardized Normal cdf.

It is worth noting that if  $X_l$  and  $X_t$  are supposed to be Normal distributed, then hypothesis 7) is violated. According to what suggested in Section 2.1, in order to fulfill hypothesis 7), the Normal distributions must be properly truncated and the limits of the truncated distributions can be considered as new parameters to be estimated. However, as it will be shown in Sections 4.4 and 4.6, the truncation can be avoided by sufficiently spacing far apart  $\mu_{X_l}$  and  $\mu_{X_t}$ : if the two location

parameters are quite distant from each other, then the probability of having  $X_t > X_l$  becomes negligible.

In the literature<sup>17,18,30</sup> different types of continuous distribution have been proposed for the number of cycles to failure. Usually, either a 2-parameter Weibull distribution or a Log-Normal distribution are used for the cycles to failure rv. In both cases the conditional fatigue life, which can be assumed to be the logarithm of the cycles to failure, follows a location-scale distribution. Without loss of generality, in the following the conditional fatigue life rv's are supposed to be Normal distributed. Therefore, suppose that  $Y|_{int}$  has location parameter  $\mu_{Y|_{int}}$  and scale parameter  $\sigma_{Y|_{int}}$ , and that  $Y|_{surf}$  has location parameter  $\mu_{Y|_{surf}}$  and scale parameter  $\sigma_{Y|_{surf}}$ , then:

$$F_{Y|_{int}} = \Phi \left[ \frac{y - \mu_{Y|_{int}}}{\sigma_{Y|_{int}}} \right], \quad (9)$$

and

$$F_{Y|_{surf}} = \Phi \left[ \frac{y - \mu_{Y|_{surf}}}{\sigma_{Y|_{surf}}} \right]. \quad (10)$$

It is well-known that the parameters of the cdf's given in Equations (9) and (10) depend on the applied stress amplitude. In particular, any monotonic decreasing function of  $x$  can be adopted for the location parameters, while, in the case of the scale parameters, any positive function can be used. In the simplest case, the scale parameters are constant and the location parameters are linear<sup>15,16,30</sup> function of the applied stress amplitude:

$$\mu_{Y|_{int}} = a_{Y|_{int}} + x \cdot b_{Y|_{int}},$$

and

$$\mu_{Y|_{surf}} = a_{Y|_{surf}} + x \cdot b_{Y|_{surf}},$$

where  $a_{Y|_{int}}$ ,  $b_{Y|_{int}}$ ,  $a_{Y|_{surf}}$  and  $b_{Y|_{surf}}$  are four constant coefficients.

In this particular case, by taking into account Equations (7-10),  $F_Y$  finally becomes:

$$F_Y = \Phi \left[ \frac{y - (a_{Y|_{surf}} + x \cdot b_{Y|_{surf}})}{\sigma_{Y|_{surf}}} \right] \Phi \left[ \frac{x - \mu_{X_t}}{\sigma_{X_t}} \right] + \Phi \left[ \frac{y - (a_{Y|_{int}} + x \cdot b_{Y|_{int}})}{\sigma_{Y|_{int}}} \right] \Phi \left[ \frac{x - \mu_{X_l}}{\sigma_{X_l}} \right] \left( 1 - \Phi \left[ \frac{x - \mu_{X_t}}{\sigma_{X_t}} \right] \right), \quad (11)$$

and the total number of parameters of the model is equal to 10.

### 3. General S-N curve

As a general rule, S-N curves can show a fatigue limit and more than two failure modes (i.e., more than one transition stress). Moreover, each failure mode can be due to more than one cause of failure (i.e., different fatigue life distributions coexist in the range between two different transition stresses): this is the case of general S-N curves. Figure 3 shows a case of S-N curve with the fatigue limit and three failure modes, each of them due to two distinct causes: as an example, internal nucleation (failure mode 1) can be due to porosity (failure cause 1<sub>1</sub>) or inclusions (failure cause 2<sub>1</sub>),

subsurface nucleation (failure mode 2) can be due to two different inclusion sizes (failure causes  $1_2$  and  $2_2$ ), and surface nucleation (failure mode 3) can be due to scratches (failure cause  $1_3$ ) or voids (failure cause  $2_3$ ).

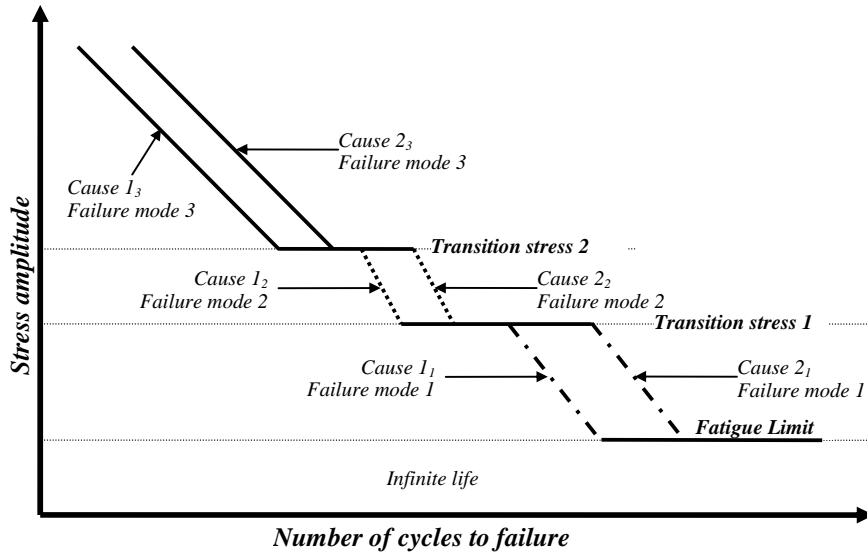


**Figure 3:** S-N curve with fatigue limit and three failure modes due to two distinct causes; causes I and II are specific to each failure mode.

The statistical fatigue life model for general S-N curves and its defining parameters are described in the following sections.

### 3.1 General S-N curve: statistical fatigue life model

The results shown in Section 2.1 can be generalized. It is possible to obtain the statistical model for general S-N curves characterized by  $m$  different failure modes and a fatigue limit. In case of general S-N curves, the hypotheses given in Section 2.1 become:

- 1) the fatigue limit,  $X_l$ , is a continuous rv;
- 2) the transition stresses,  $X_{t_1}, X_{t_2}, \dots, X_{t_{m-1}}$ , are continuous rv's;
- 3)  $X_l, X_{t_1}, X_{t_2}, \dots, X_{t_{m-1}}$  are mutually independent rv's;
- 4) the failure mode,  $M$ , is a discrete rv with realizations  $1, \dots, i, \dots, m$ ;
- 5) the failure causes,  $C_1, \dots, C_i, \dots, C_m$ , are discrete rv's;
- 6) possible realizations of the  $i$ -th failure cause (i.e., the rv,  $C_i$ , representing all failure causes generating the  $i$ -th failure mode) are  $1, \dots, j, \dots, c_i$  with probability equal to  $p_{1|i}, \dots, p_{j|i}, \dots, p_{c_i|i}$ , respectively;
- 7) the fatigue life given that  $M = i$  and  $C_i = j$  is a conditional rv,  $Y|(i, j)$ , with cdf  $F_{Y|(i, j)}$ ;
- 8) the event  $X_l \leq X_{t_1} \leq X_{t_2} \leq \dots \leq X_{t_{m-1}}$  is almost sure.

As shown in Figure 4, hypothesis 8) can be graphically visualized with a stress amplitude axis representation concerning a single specimen.

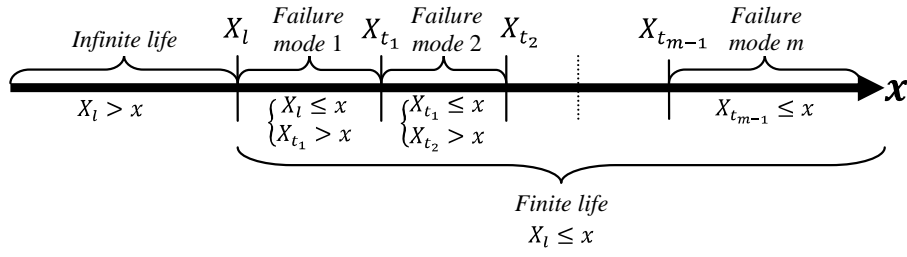


**Figure 4:** Stress amplitude axis representation of hypothesis 8); general S-N curve.

According to hypotheses 3) and 8) and with reference to Figure 4, it is possible to determine the probability of having a specimen that fails with failure mode 1:

$$P[M = 1] = P[X_l \leq x, X_{t_1} > x] = F_{X_l} (1 - F_{X_{t_1}}). \quad (12)$$

With similar considerations, the probability that a specimen fails with the  $i$ -th failure mode is given by:

$$P[M = i] = P[X_{t_{i-1}} \leq x, X_{t_i} > x] = F_{X_{t_{i-1}}} (1 - F_{X_{t_i}}), \quad (13)$$

and the probability of having a specimen that fails with the  $m$ -th failure mode is given by:

$$P[M = m] = P[X_{t_{m-1}} \leq x] = F_{X_{t_{m-1}}}. \quad (14)$$

By letting  $F_{X_{t_0}} = F_{X_l}$  and  $F_{X_{t_m}} = 0$ , Equations (12) and (14) become particular cases of Equation (13).

By focusing on the  $i$ -th failure mode, the probability that a specimen fails with failure mode  $i$  for the  $j$ -th failure cause is given by:

$$P[M = i, C_i = j] = P[C_i = j | M = i] \cdot P[M = i] = p_{j|i} F_{X_{t_{i-1}}} (1 - F_{X_{t_i}}).$$

The probability that a specimen fails with the  $i$ -th failure mode for the  $j$ -th failure cause and with a fatigue life smaller than  $y$  is therefore given by:

$$\begin{aligned} P[Y \leq y, M = i, C_i = j] &= P[Y \leq y | (M = i, C_i = j)] \cdot P[M = i, C_i = j] = \\ &= F_{Y|(i,j)} p_{j|i} F_{X_{t_{i-1}}} (1 - F_{X_{t_i}}). \end{aligned}$$

Similarly to what stated for the failure modes in Section 2.1, the  $c_i$  failure causes form a partition of the  $i$ -th failure mode. As an easy application of the Total Probability, it follows that the probability of having a failure with failure mode  $i$  and with fatigue life smaller than  $y$  is therefore given by:

$$P[Y \leq y, M = i] = F_{X_{t_{i-1}}} (1 - F_{X_{t_i}}) \sum_{j=1}^{c_i} F_{Y|(i,j)} p_{j|i}.$$

What demonstrated for two failure modes in Section 2.1 can be easily extended to the case of more than two failure modes. Indeed, it can be shown that, according to the hypotheses 3) and 8),

the  $m$  failure modes form a partition of the set of finite lives. Therefore, by taking into account the Total Probability Theorem, the cdf of  $Y$  is finally given by:

$$F_Y = \sum_{i=1}^m F_{X_{t_{i-1}}} \left(1 - F_{X_{t_i}}\right) \sum_{j=1}^{c_i} F_{Y|(i,j)} p_{j|i}, \quad (15)$$

which represents the statistical fatigue life model for general S-N curves.

### 3.2. General S-N curve: parameters

In case of general S-N curves,  $m$  generalized transition stresses (i.e., rv's that are either transition stresses or fatigue limit) are present in the model. According to what stated in Section 2.2 and without loss of generality, the generic  $X_{t_{i-1}}$  rv is supposed to be Normal distributed:

$$F_{X_{t_{i-1}}} = \Phi \left[ \frac{x - \mu_{X_{t_{i-1}}}}{\sigma_{X_{t_{i-1}}}} \right], \quad (16)$$

with  $\mu_{X_{t_0}} = \mu_{X_l}$  and  $\sigma_{X_{t_0}} = \sigma_{X_l}$ .

Similarly, the generic conditional cdf,  $F_{Y|(i,j)}$ , is given by:

$$F_{Y|(i,j)} = \Phi \left[ \frac{y - \mu_{Y|(i,j)}}{\sigma_{Y|(i,j)}} \right]. \quad (17)$$

In the most simple case, the location parameters linearly depend on the applied stress amplitude and the scale parameters are constant. In this case, Equation (17) becomes:

$$F_{Y|(i,j)} = \Phi \left[ \frac{y - (a_{Y|(i,j)} + b_{Y|(i,j)} \cdot x)}{\sigma_{Y|(i,j)}} \right]. \quad (18)$$

Finally, the conditional probabilities  $p_{j|i}$  must be considered. For each failure mode, the  $p_{j|i}$  must sum to unity (i.e.,  $\sum_{j=1}^{c_i} p_{j|i} = 1$ ). Therefore the number of  $p_{j|i}$  that must be known is  $\sum_{i=1}^m (c_i - 1)$ .

If models (16) and (18) hold, then Equation (15) becomes:

$$F_Y = \sum_{i=1}^m \Phi \left[ \frac{x - \mu_{X_{t_{i-1}}}}{\sigma_{X_{t_{i-1}}}} \right] \left( 1 - \Phi \left[ \frac{x - \mu_{X_{t_i}}}{\sigma_{X_{t_i}}} \right] \right) \sum_{j=1}^{c_i} \Phi \left[ \frac{y - (a_{Y|(i,j)} + b_{Y|(i,j)} \cdot x)}{\sigma_{Y|(i,j)}} \right] p_{j|i},$$

and the total number of parameters involved in model (15) is given by:

$$n_{par} = 2m + 3 \sum_{i=1}^m c_i + \sum_{i=1}^m (c_i - 1). \quad (19)$$

If  $m = 2$  and  $c_1 = c_2 = 1$ , to say, there are 2 failure modes and 1 failure cause for each failure mode, Equation (19) gives  $n_{par} = 10$ , which confirms the result obtained in Section 2.2.

## 4. Numerical examples

Fatigue data plots available in the literature are very different. In the following, it will be shown that they can be qualitatively described by the general model (15) with suitable hypotheses on the

parameters. The aim of the present paper is statistical modeling rather than statistical fitting and, as a consequence, the values considered for the parameters are arbitrarily assumed for qualitative purposes. Well-known statistical methods for parameter estimation (e.g., graphical methods and the Maximum Likelihood principle) can be adopted for quantitatively fitting the general model (15) to the experimental data. Indeed, if applied, fitting of experimental data would permit to estimate at once different key material parameters and, consequently, to make assumptions about the presence of a fatigue limit (with its mean value and scatter), and of a transition stress (with its mean value and scatter), and to potentially distinguish between two distinct failure modes (e.g., surface-initiated or internal-initiated failure) or failure causes (e.g., two types of inclusion with significantly different sizes) prior to any fractographic analysis. For instance, if two types of inclusion with significantly different sizes originated the same internal failure mode, then the final distribution for the fatigue life is expected to be bimodal with scatter significantly influenced by the two original statistical populations of inclusion size. Therefore, fitting of experimental data would give a bimodal fatigue life distribution model, which could give to the experimenter an indication about the type of distributions which originated the fatigue life data.

#### 4.1 One failure mode due to one cause without fatigue limit

This is the most simple case, with  $m = 1$ ,  $c_1 = 1$  and  $F_{X_{t_0}} = F_{X_l} = 1$ . According to Sections 3.1 and 3.2,  $F_{X_{t_m}} = 0$  and  $\sum_{j=1}^{c_i} P_{j|i} = 1$ . Since  $m = 1$  and  $c_1 = 1$ , it follows that  $P_{1|1} = 1$  and  $F_{X_{t_1}} = 0$ , and the final model is given by:

$$F_Y = F_{Y|(1,1)}. \quad (20)$$

If Equation (18) is considered, then Equation (20) is in agreement with the linear models proposed in the literature and in international standards<sup>15,16</sup> and the final model depends on the 3 parameters,  $a_{Y|(1,1)}$ ,  $b_{Y|(1,1)}$  and  $\sigma_{Y|(1,1)}$ . As an example, let  $a_{Y|(1,1)}$  be equal to 20,  $b_{Y|(1,1)}$  be equal to  $-1$  and  $\sigma_{Y|(1,1)}$  be equal to 0.5. With these hypotheses, model (20) finally becomes:

$$F_Y = \Phi \left[ \frac{y - (20 - x)}{0.5} \right]. \quad (21)$$

Figure 5a shows the S-N curves obtained by using model (21) with failure probabilities equal to 0.1, 0.5 and 0.9, respectively. As shown in Figure 5b, the cdf's at two different  $x$  values are only shifted, since  $\sigma_{Y|(1,1)}$  is supposed constant.

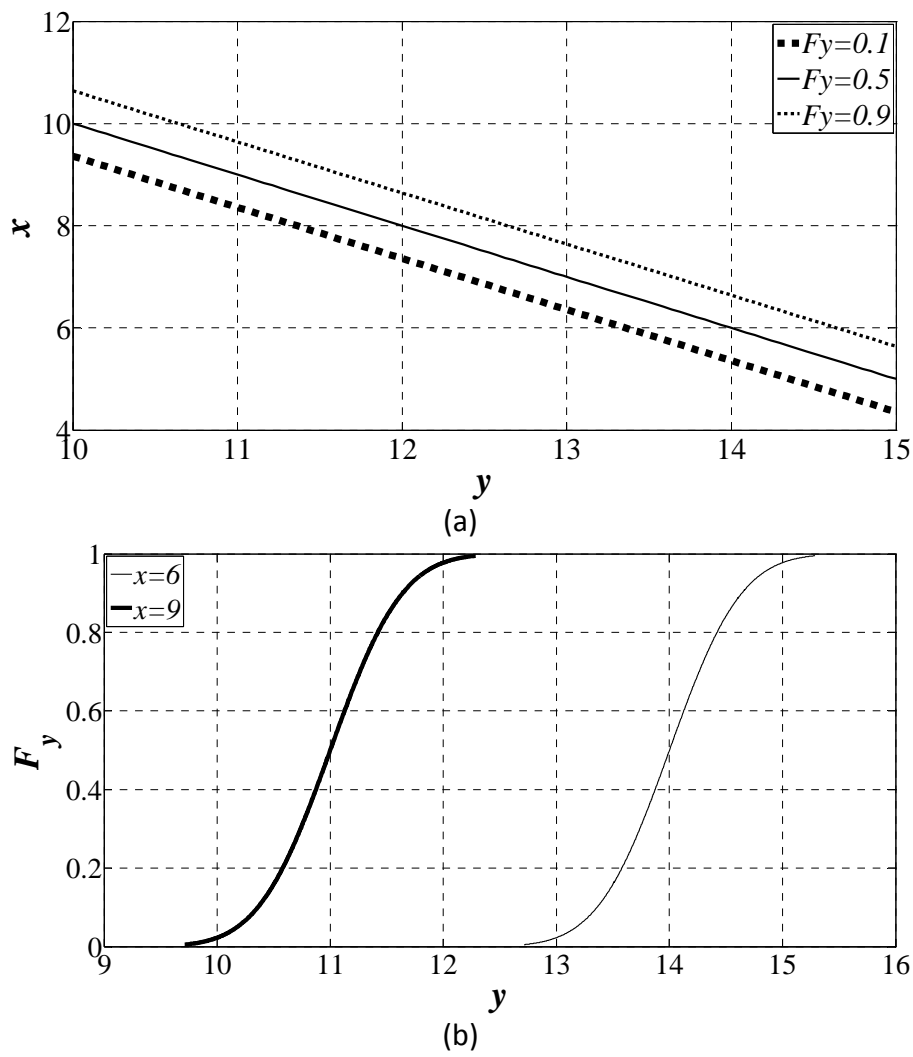
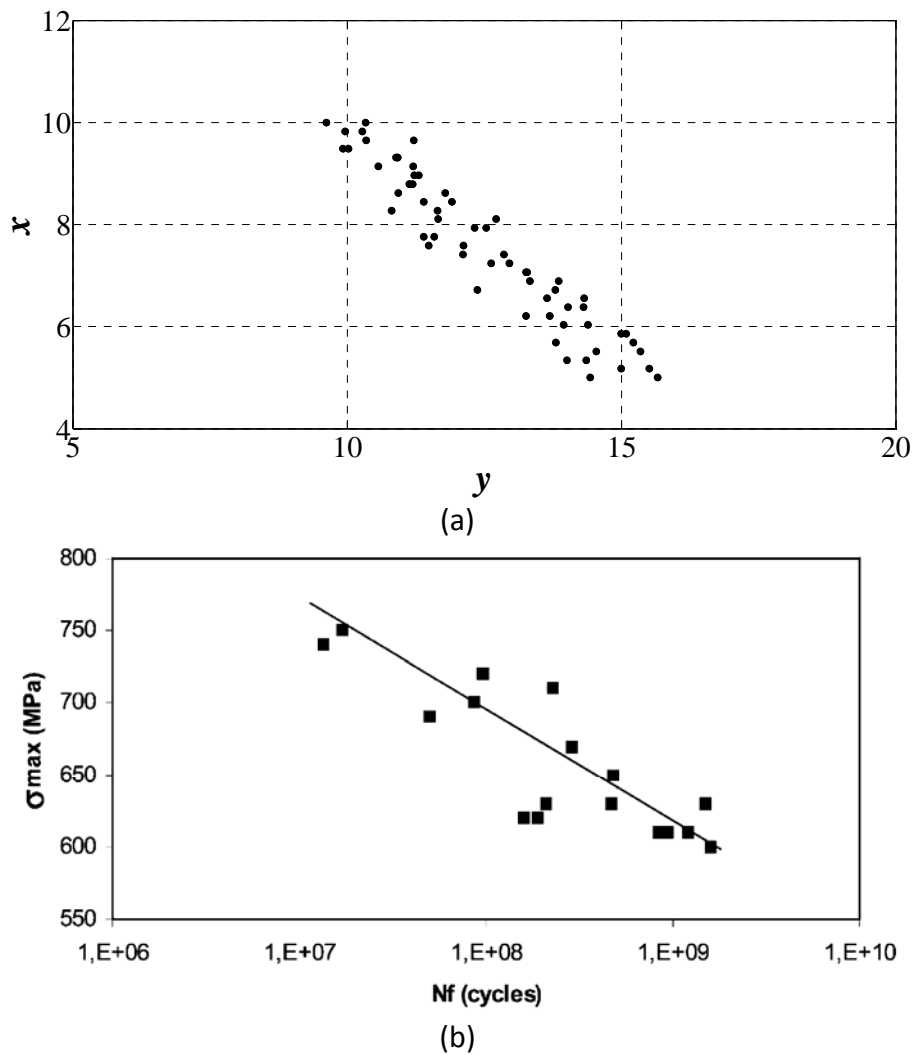


FIGURE 5

**Figure 5:** (a) S-N curves calculated from model (21) for different failure probabilities. (b) Cdf's of  $Y$  for different values of applied stress amplitude.

Figure 6 shows the good qualitative agreement between random data (Figure 6a) generated from model (21) and, e.g., experimental data (Figure 6b) obtained on 17-4PH martensitic stainless steel specimens<sup>31</sup>.



**Figure 6:** (a) Random generated data from model (21). (b) Experimental fatigue data plot<sup>31</sup>.

Random data are generated by considering 30 equispaced values of  $x$  varying from 5 to 10. For each value of  $x$ , 2 random probability values are generated. If  $q_{i,rand}$  denotes the  $i$ -th random probability value, then the equation  $F_Y[y_{i,rand}] = q_{i,rand}$  allows to compute the  $i$ -th random fatigue life value,  $y_{i,rand}$ . By repeating the procedure for each  $q_{i,rand}$  value, the set of random data used for Figure 6a can be finally obtained. In the following numerical examples, a similar procedure is adopted to generate random data resembling experimental data taken from the open literature. The number of generated random data is different for Subsections 4.1-4.7; the random data plots (Figures 6, 8, 10, 12, 14, 16, 18 and 20) show that the proposed statistical model is not affected by the variation in data numerosity. Furthermore, it is worth noting that no attempt is made to quantitatively reproduce experimental data: graphs with random generated data aim only to show the potentiality of the proposed statistical model in catching possible qualitative trends of experimental data taken from the open literature. For this reason, figures with random generated data have axes, intentionally indicated with generic symbols “ $x$ ” and “ $y$ ”, which may be different from the axes of the corresponding figures with experimental data.



## 4.2 One failure mode due to one cause with fatigue limit

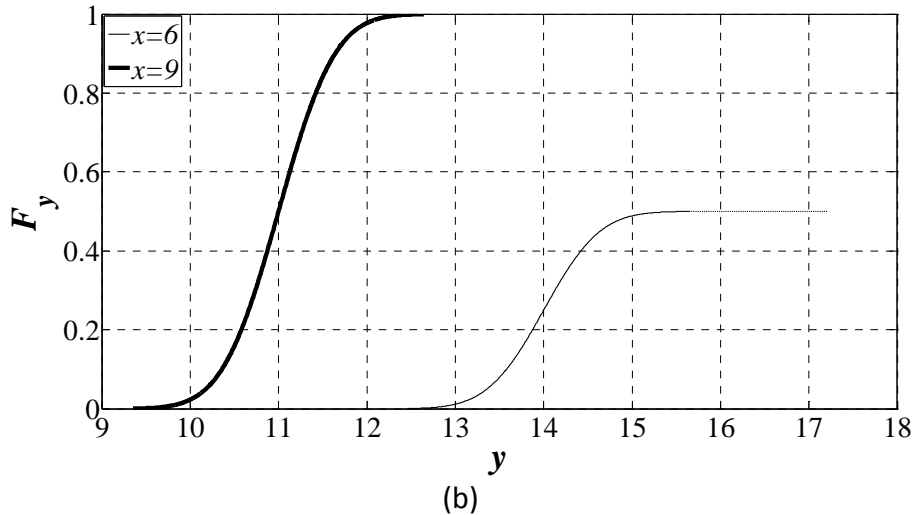
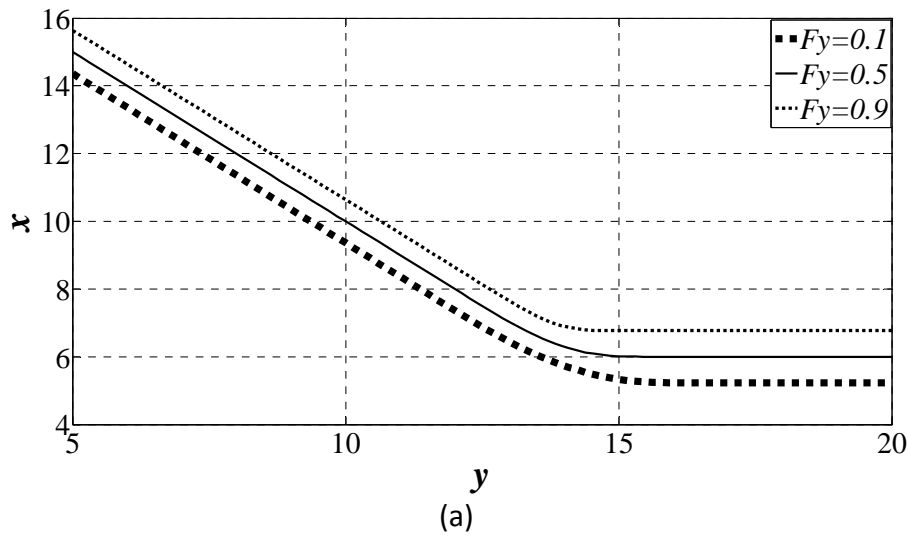
As in the previous case,  $m = 1$  and  $c_1 = 1$ . However, differently from what stated in Section 4.1,  $F_{X_l}$  is smaller than 1. According to these hypotheses model (15) becomes:

$$F_Y = F_{X_l} F_{Y|(1,1)}. \quad (22)$$

If Equations (16) and (18) are considered, then the cdf (22) depends on 5 parameters and corresponds to models already proposed in the literature<sup>17,18</sup>. As an example, let  $\mu_{X_l}$  be equal to 6,  $\sigma_{X_l}$  be equal to 0.6, the other 3 parameters be equal to the values given in Section 4.1, then model (22) becomes:

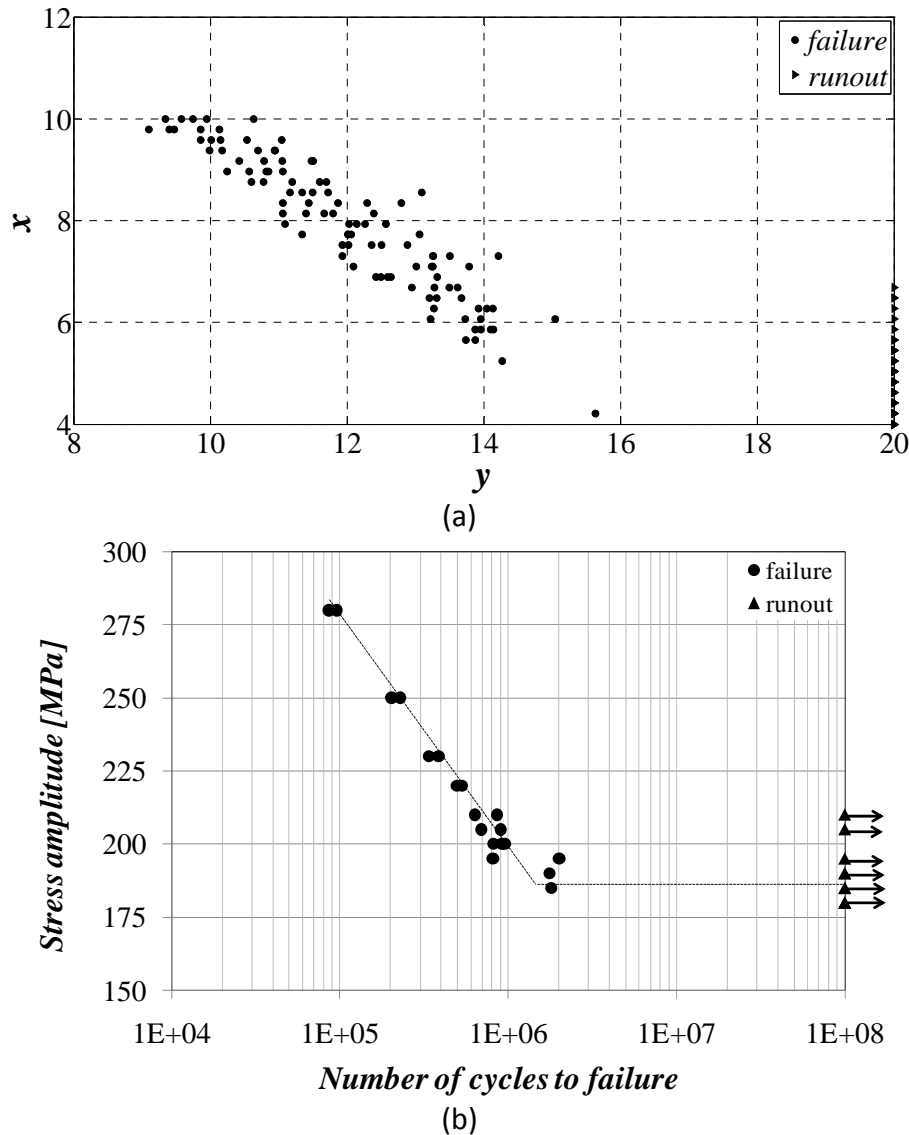
$$F_Y = \Phi \left[ \frac{x-6}{0.6} \right] \Phi \left[ \frac{y-(20-x)}{0.5} \right]. \quad (23)$$

Figure 7a shows the S-N curves obtained by using model (23) with failure probabilities equal to 0.1, 0.5 and 0.9, respectively. As shown in Figure 7b, the cdf's at two different  $x$  values are different due to the presence of  $F_{X_l}$ . In particular, if the cdf at  $x = 6$  is considered, the number of cycles to failure is infinite for values of  $F_Y$  larger than  $\Phi \left( \frac{6-6}{0.6} \right) = 0.5$  while, if the cdf at  $x = 9$  is considered, the number of cycles to failure is infinite for values of  $F_Y$  larger than  $\Phi \left( \frac{9-6}{0.6} \right) \cong 1$ .



**Figure 7:** (a) S-N curves calculated from model (23) for different failure probabilities. (b) Cdf's of  $Y$  for different values of  $x$ .

Figure 8 shows the good qualitative agreement between random data (Figure 8a) generated by using model (23) and experimental data (Figure 8b) obtained, e.g., on JIS-SUS403B stainless steel specimens<sup>32</sup> with stress concentration factor equal to 2 and tested at 300 °C.



**Figure 8:** (a) Random generated data from model (23). (b) Experimental fatigue data plot<sup>32</sup>.

Random data are generated by considering 30 equispaced values of  $x$  varying from 4 to 10. For each value of  $x$ , 5 random values are generated with the procedure explained in Section 4.1. In this case, if  $q_{i,rand}$  is larger than the corresponding value of  $F_{X_l}$ , then  $y_{i,rand}$  is set equal to infinite (i.e., the value of  $x$  is below the fatigue limit and the fatigue life becomes infinite).

### 4.3 Two failure modes due to one cause without plateau and fatigue limit

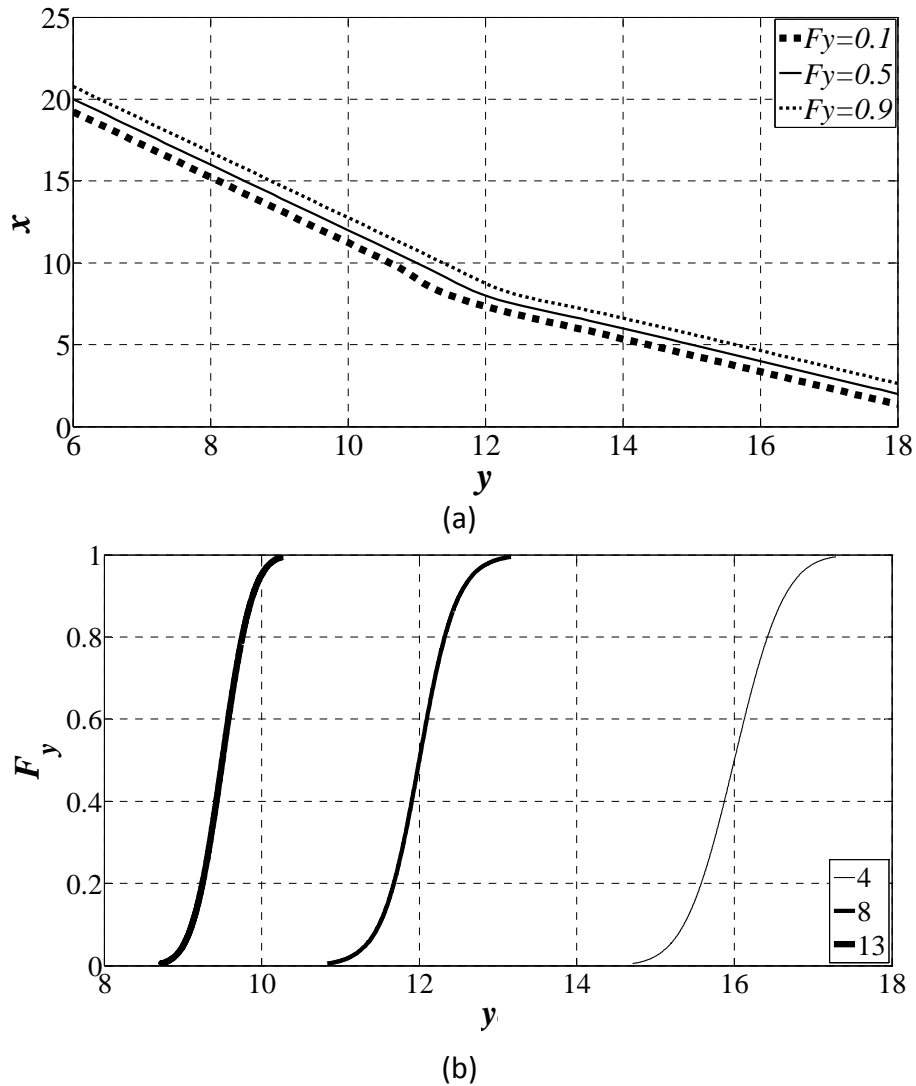
In this case,  $m = 2$  and  $c_1 = c_2 = 1$ . Since the fatigue limit is absent,  $F_{X_{t_0}} = F_{X_l} = 1$ . According to what stated in Sections 3.1 and 3.2,  $F_{X_{t_m}} = 0$  and  $\sum_{j=1}^{c_i} P_{j|i} = 1$ . Since  $m = 2$  and  $c_1 = c_2 = 1$ , it follows that  $P_{1|1} = P_{1|2} = 1$  and  $F_{X_{t_2}} = 0$ , and the final model is given by:

$$F_Y = \left(1 - F_{X_{t_1}}\right) F_{Y|(1,1)} + F_{X_{t_1}} F_{Y|(2,1)}. \quad (24)$$

If Equations (16) and (18) are considered, then the cdf (24) depends on 8 parameters. As an example, let  $\mu_{X_{t_1}}$  be equal to 8,  $\sigma_{X_{t_1}}$  be equal to 0.8,  $a_{Y|(2,1)}$  be equal to 16,  $b_{Y|(2,1)}$  equal to  $-0.5$  and  $\sigma_{Y|(2,1)}$  equal to 0.3, the last 3 parameters be equal to the values given in Section 4.1, then model (24) becomes:

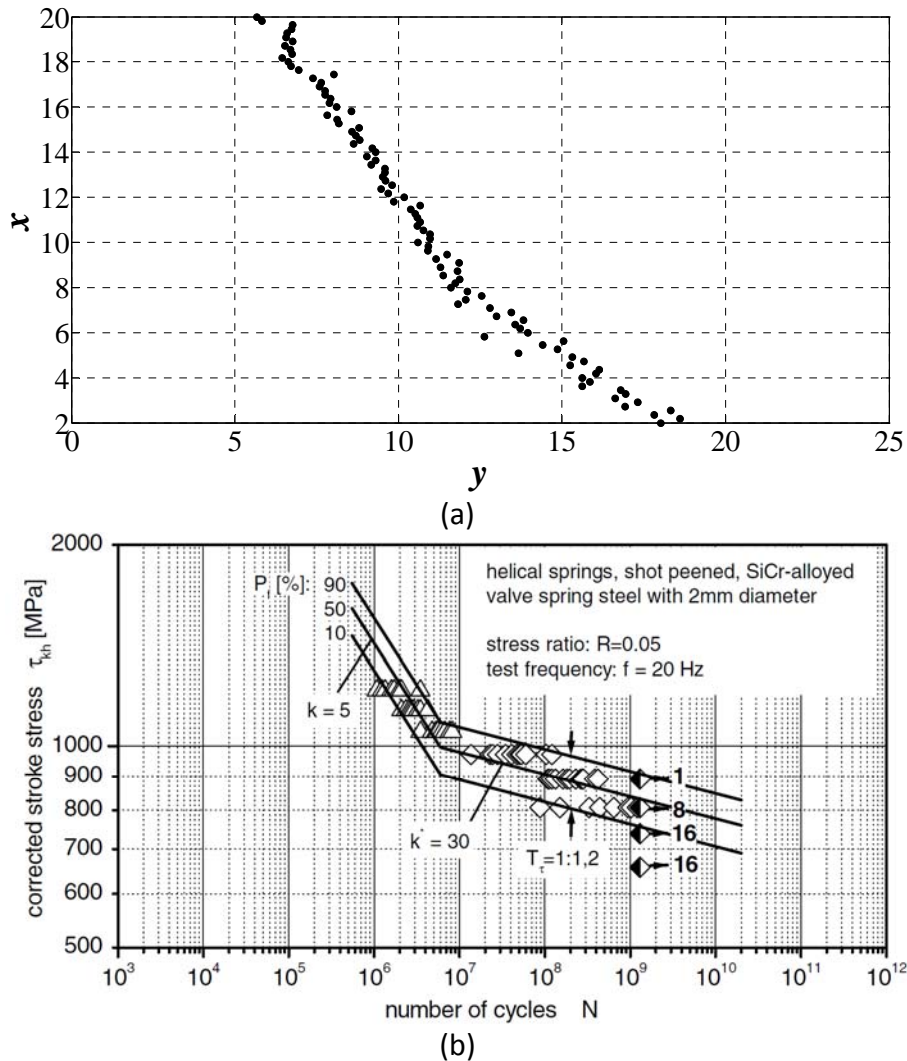
$$F_Y = \left(1 - \Phi \left[\frac{x-8}{0.8}\right]\right) \Phi \left[\frac{y-(20-x)}{0.5}\right] + \Phi \left[\frac{x-8}{0.8}\right] \Phi \left[\frac{y-(16-0.5x)}{0.3}\right]. \quad (25)$$

Figure 9a shows the S-N curves obtained by using model (25) with failure probabilities equal to 0.1, 0.5 and 0.9, respectively. As shown in Figure 9b, the cdf's at three different  $x$  values are shifted and have different standard deviations. In particular, if the cdf at  $x = 4$  is considered, the standard deviation is close to  $\sigma_{Y|(1,1)} = 0.5$  while, if the cdf at  $x = 13$  is considered, the standard deviation reduces and is close to  $\sigma_{Y|(2,1)} = 0.3$ .



**Figure 9:** (a) S-N curves calculated from model (25) for different failure probabilities. (b) Cdf's of  $Y$  for different values of  $x$ .

Figure 10 shows the good qualitative agreement between random data (Figure 10a) generated by using model (25) and experimental data (Figure 10b) obtained, e.g., on shot-peened helical compression springs<sup>33</sup>.



**Figure 10:** (a) Random generated data from model (25). (b) Experimental fatigue data plot<sup>33</sup>.

Random data are generated by considering 100 equispaced values of  $x$  varying from 2 to 20. For each value of  $x$ , 1 random fatigue life value is generated with the procedure explained in Section 4.1.

#### 4.4 Two failure modes due to one cause without plateau and with fatigue limit

As in the previous case,  $m = 2$  and  $c_1 = c_2 = 1$ . However, differently from what stated in Section 4.3,  $F_{X_l}$  is smaller than 1. According to these hypotheses model (15) becomes equal to model (11):

$$F_Y = F_{X_l} \left( 1 - F_{X_{t_1}} \right) F_{Y|(1,1)} + F_{X_{t_1}} F_{Y|(2,1)}. \quad (26)$$

If Equations (16) and (18) are considered, then cdf (26) depends on 10 parameters. As an example, let  $\mu_{X_l}$  be equal to 2,  $\sigma_{X_l}$  be equal to 0.3, the other 8 parameters be equal to the values given in Section 4.3, then model (26) becomes:

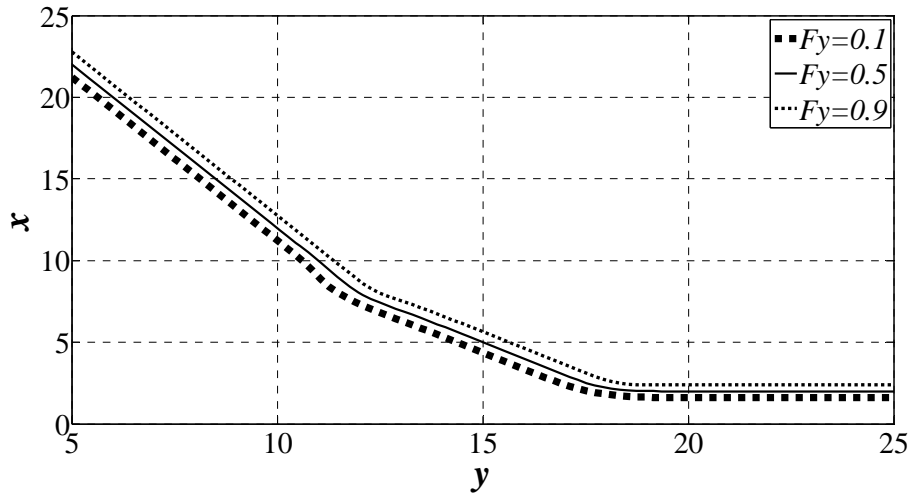
$$F_Y = \Phi \left[ \frac{x-2}{0.3} \right] \left( 1 - \Phi \left[ \frac{x-8}{0.8} \right] \right) \Phi \left[ \frac{y-(20-x)}{0.5} \right] + \Phi \left[ \frac{x-8}{0.8} \right] \Phi \left[ \frac{y-(16-0.5x)}{0.3} \right]. \quad (27)$$

It must be pointed out that, if a Normal distribution is assumed for both  $X_l$  and  $X_{t_1}$ , then hypothesis 7) of Section 3.1 is violated. Nevertheless the violation is negligible since the probability of having  $X_l \leq X_{t_1}$  is given by:

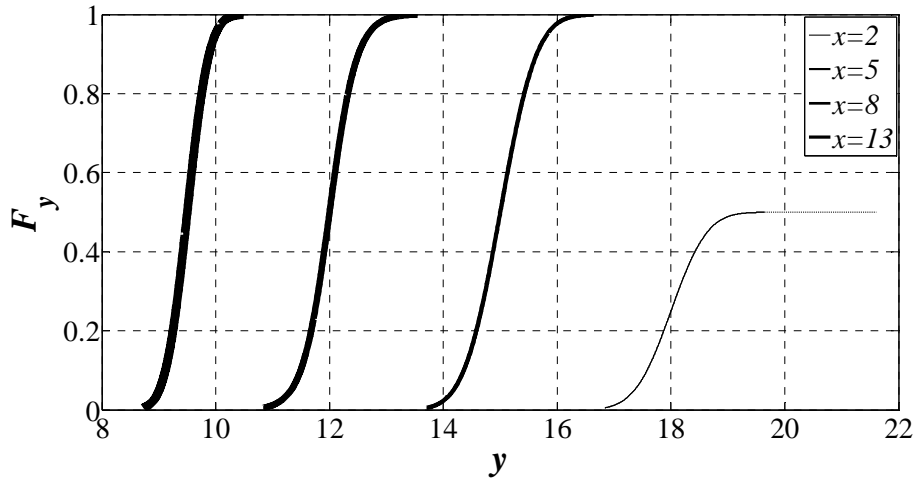
$$P[X_l - X_{t_1} \leq 0] = \Phi \left[ \frac{0-(2-8)}{\sqrt{0.3^2+0.8^2}} \right] \cong \Phi[7] \cong 1,$$

being  $X_l$  and  $X_{t_1}$  independent and Normal distributed. It is worth noting that if the violation is not negligible, then it is possible to limit the two distributions as suggested in Section 2.1. Nevertheless, in real cases<sup>1,5,6</sup> the distance between the location parameters of the two distributions is large and violations are in most cases negligible.

Figure 11a shows the S-N curves obtained by using model (27) with failure probabilities equal to 0.1, 0.5 and 0.9, respectively. As shown in Figure 11b, the cdf's at four different  $x$  values are different. In particular, if the cdf at  $x = 2$  is considered, the number of cycles to failure is infinite for values of  $F_Y$  larger than  $\Phi \left[ \frac{2-2}{0.3} \right] = 0.5$  while, in the other cases, the number of cycles to failure is infinite when  $F_Y$  is close to 1.



(a)



(b)

**Figure 11:** (a)  $S-N$  curves calculated from model (27) for different failure probabilities. (b) Cdf's of  $Y$  for different values of  $x$ .

Figure 12 shows the good qualitative agreement between random data (Figure 12a) generated by using model (27) and experimental data (Figure 12b) obtained, e.g., on JIS-SUS403B stainless steel specimens<sup>32</sup> with stress concentration factor equal to 3 and tested at 500 °C.

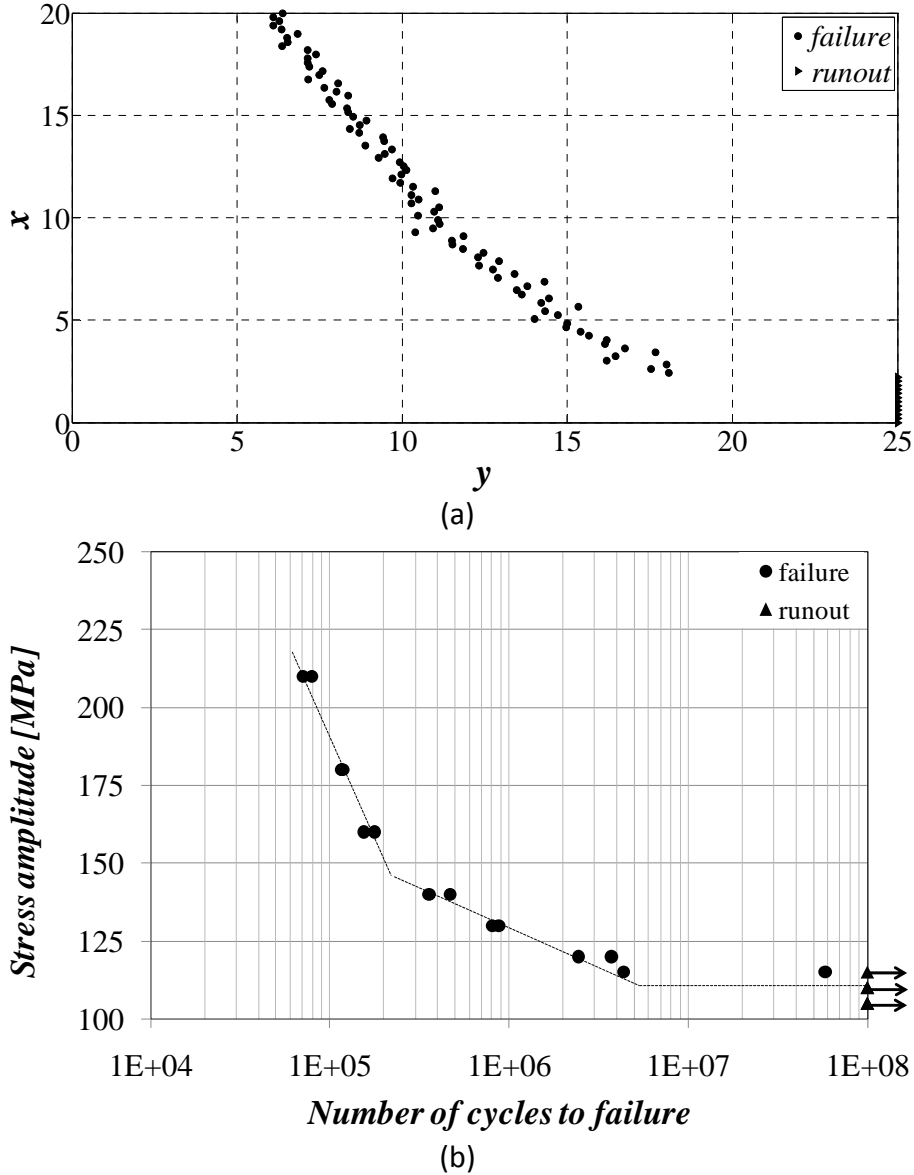


**Figure 12:** (a) Random generated data from model (27). (b) Experimental fatigue data plot<sup>32</sup>.

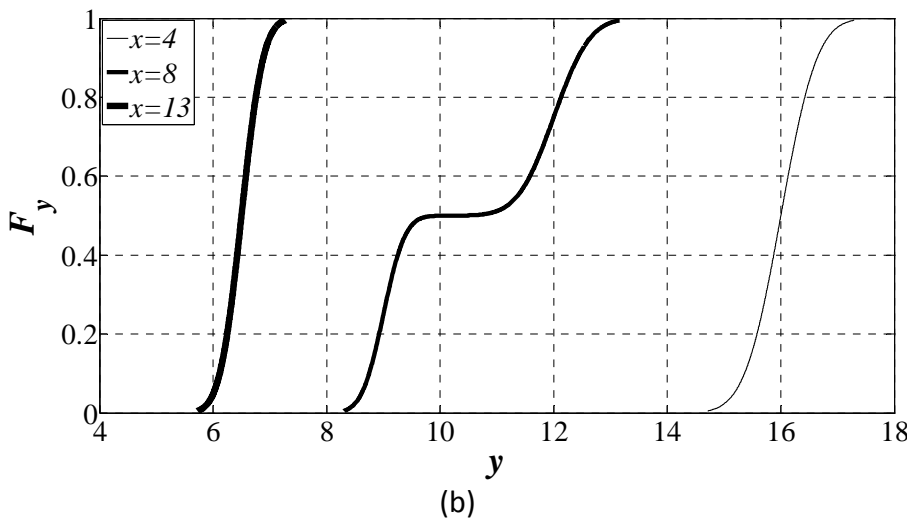
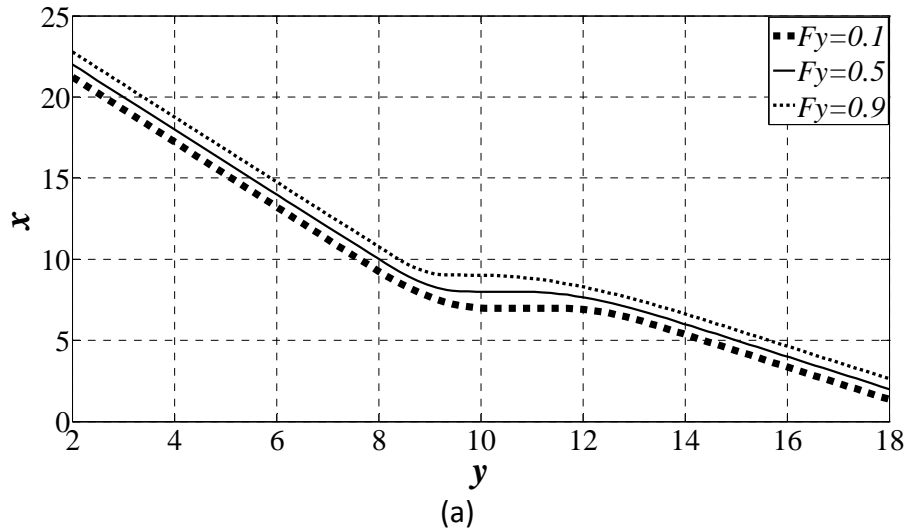
Random data are generated by considering 100 equispaced values of  $x$  varying from 0 to 20. For each value of  $x$ , 1 random fatigue life value is generated with the procedure explained in Section 4.2.

#### 4.5 Two failure modes due to one cause with plateau and without fatigue limit

Model (24) applies in this case. Except for parameter  $a_{Y|(2,1)}$  which changes and is set equal to 13, all the hypotheses considered in Section 4.4 are confirmed. Therefore, the final model becomes:

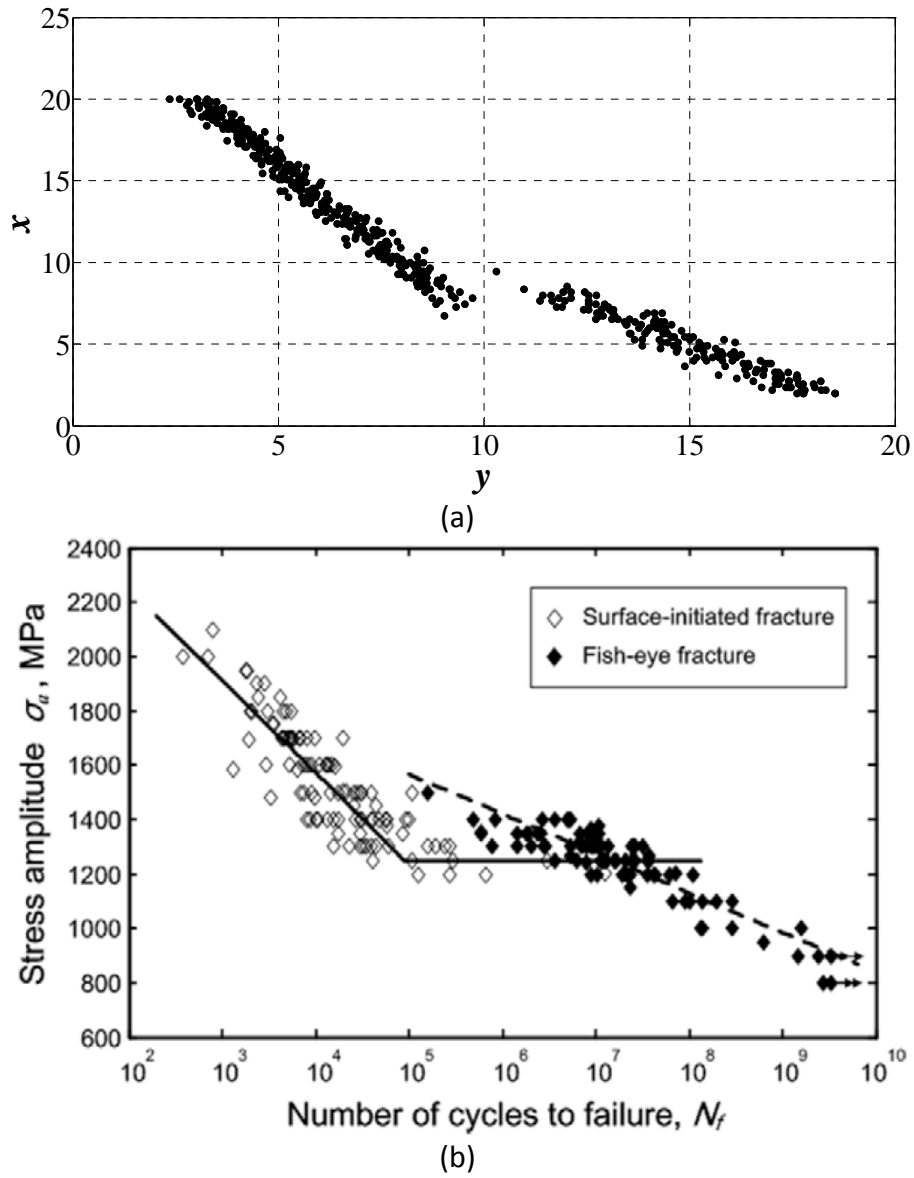
$$F_Y = \left(1 - \Phi \left[ \frac{x-8}{0.8} \right]\right) \Phi \left[ \frac{y-(20-x)}{0.5} \right] + \Phi \left[ \frac{x-8}{0.8} \right] \Phi \left[ \frac{y-(13-0.5x)}{0.3} \right]. \quad (28)$$

Figure 13a shows the S-N curves obtained by using model (28) with failure probabilities equal to 0.1, 0.5 and 0.9, respectively. As shown in Figure 13b, the cdf's at three different  $x$  values have different shapes. In particular, the cdf corresponding to  $x = 8$  has the typical shape of a mixture of distributions. Indeed, at  $x = 8$  the coexistence of the two failure modes originates a mixture of distributions and the cdf of each failure mode contributes with probability  $\Phi \left[ \frac{8-8}{0.8} \right] = 0.5$  to the cdf of  $Y$ .



**Figure 13:** (a) S-N curves calculated from model (28) for different failure probabilities. (b) Cdf's of  $Y$  for different values of  $x$ .

Figure 14 shows the good qualitative agreement between random data (Figure 14a) generated by using model (28) and experimental data (Figure 14b) obtained, e.g., on JIS-SUJ2 steel specimens<sup>6</sup>.



**Figure 14:** (a) Random generated data from model (28). (b) Experimental fatigue data plot<sup>6</sup>.

Random data are generated by considering 100 equispaced values of  $x$  varying from 2 to 20. For each value of  $x$ , 5 random fatigue life values are generated with the procedure explained in Section 4.1.

#### 4.6 Two failure modes due to one cause with plateau and with fatigue limit

Model (26) applies in this case. Except for parameters  $a_{Y|(2,1)}$ ,  $b_{Y|(2,1)}$  and  $\sigma_{Y|(2,1)}$  which change and are set equal to 24,  $-2$  and 1, respectively, all the hypotheses considered in Section 4.4 are confirmed. The final model becomes:

$$F_Y = \Phi \left[ \frac{x-2}{0.3} \right] \left( 1 - \Phi \left[ \frac{x-8}{0.8} \right] \right) \Phi \left[ \frac{y-(20-x)}{0.5} \right] + \Phi \left[ \frac{x-8}{0.8} \right] \Phi [y - (24 - 2x)]. \quad (29)$$

As shown in Section 4.4, hypothesis 7) of Section 3.1 is violated but the violation is negligible.

Figure 15a shows the S-N curves obtained by using model (29) with failure probabilities equal to 0.1, 0.5 and 0.9, respectively. As shown in Figure 15b, the cdf's at four different  $x$  values have different shapes. In particular, the cdf's corresponding to  $x = 8$  and to  $x = 10$  have the typical



shape of a mixture of distributions, while the cdf corresponding to  $x = 2$  gives infinite number of cycles to failure for values of  $F_Y$  larger than  $\Phi\left[\frac{2-2}{0.3}\right] = 0.5$ .

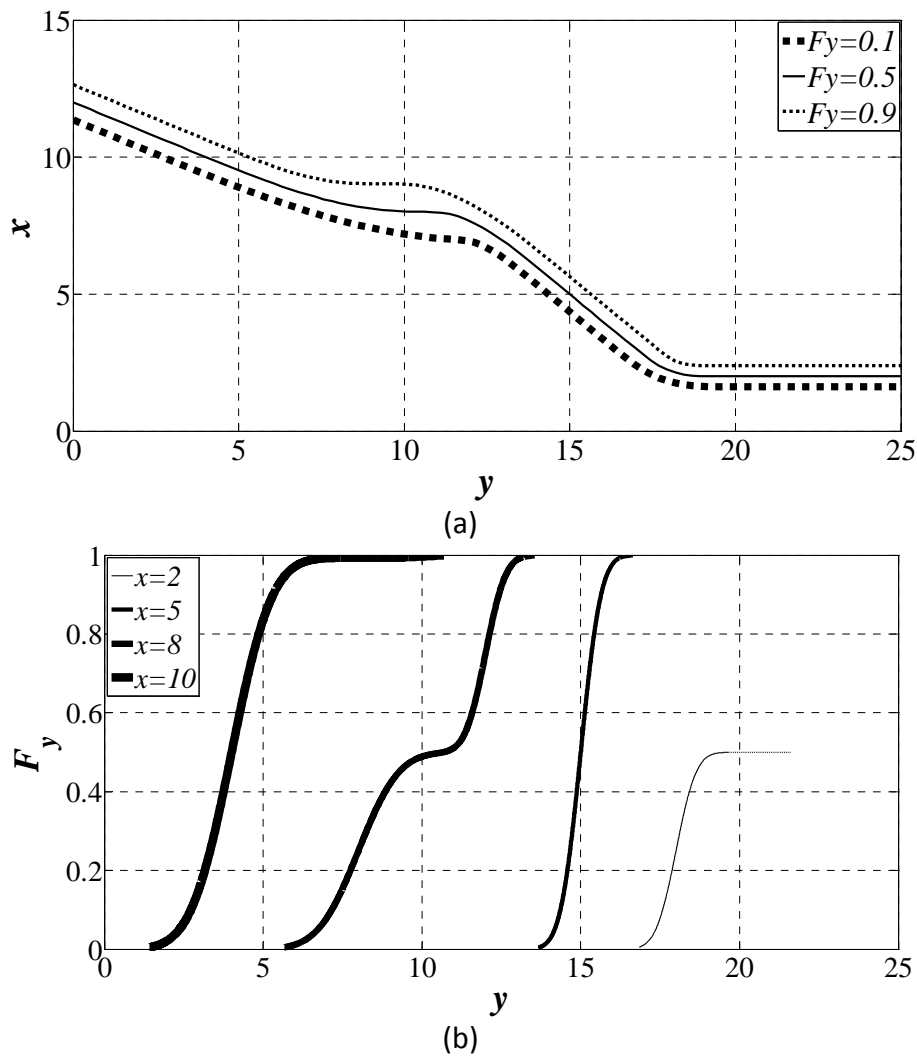


**Figure 15:** (a)  $S-N$  curves calculated from model (29) for different failure probabilities. (b) Cdf's of  $Y$  for different values of  $x$ .

Figure 16 shows the good qualitative agreement between random data (Figure 16a) generated by using model (29) and experimental data (Figure 16a) obtained, e.g., on Ti-6Al-4V titanium alloy specimens<sup>34</sup>.

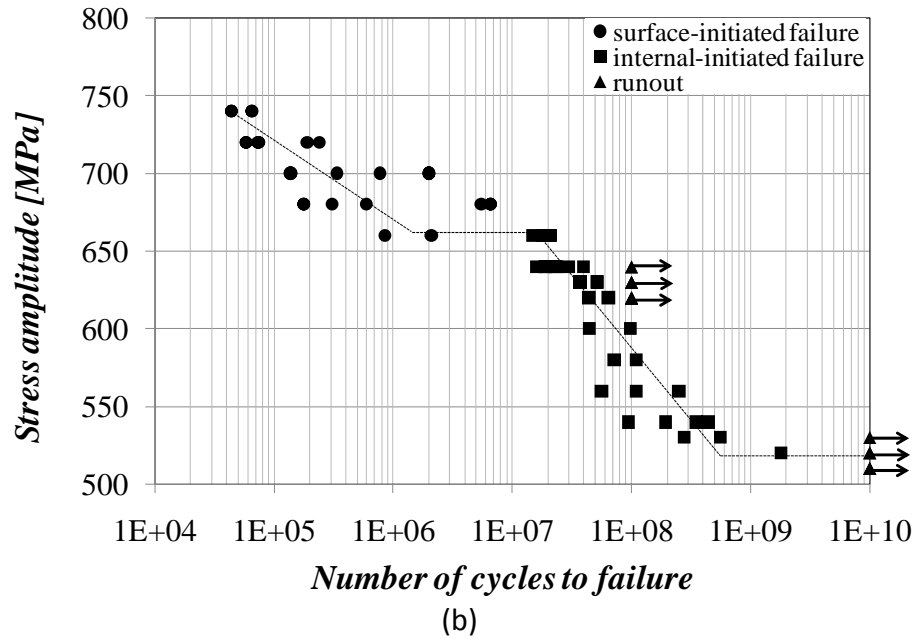
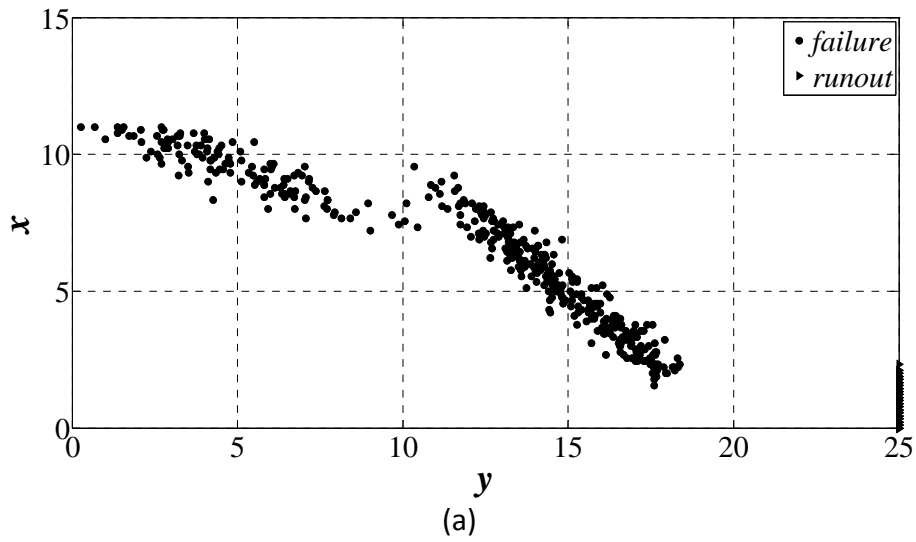


**Figure 16:** (a) Random generated data from model (29). (b) Experimental fatigue data plot<sup>34</sup>.

Random data are generated by considering 100 equispaced values of  $x$  varying from 0 to 11. For each value of  $x$ , 5 random fatigue life values are generated with the procedure explained in Section 4.2.

#### 4.7 One failure mode due to two causes without fatigue limit

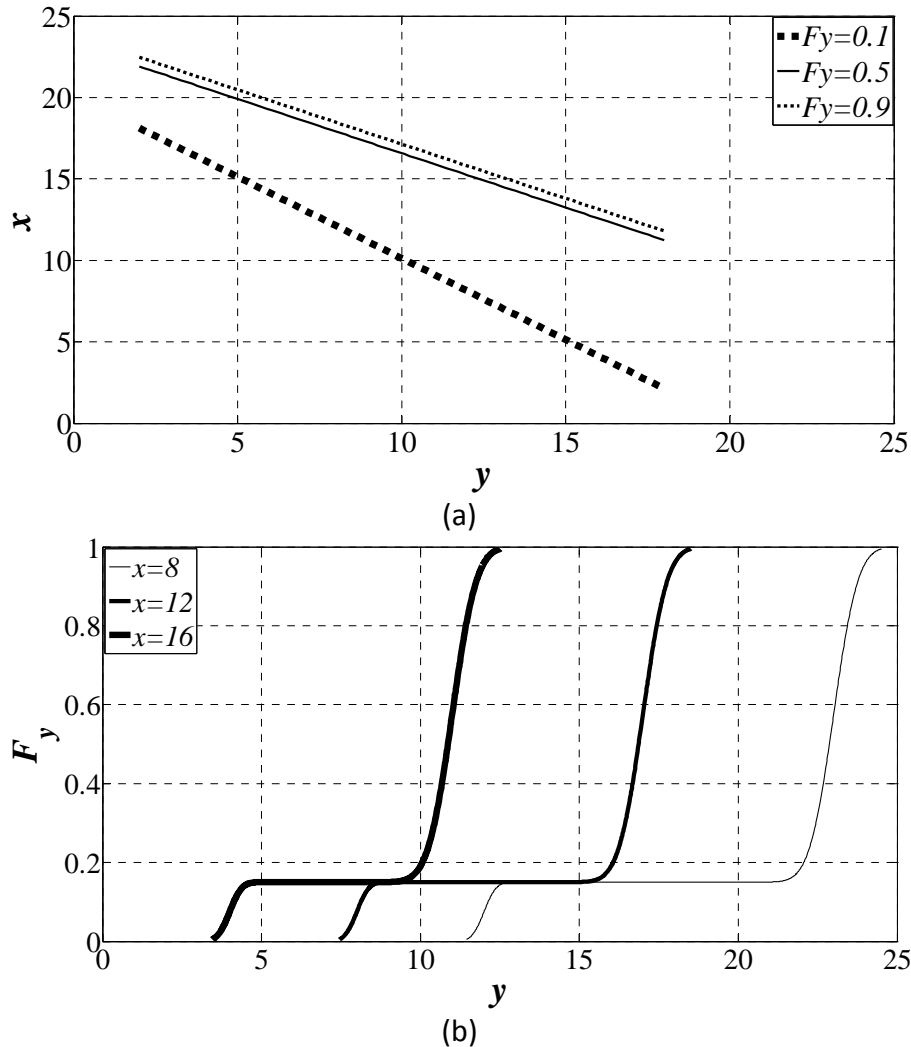
In this case,  $m = 1$ ,  $c_1 = 2$  and  $F_{x_t} = 1$ . According to what stated in Sections 3.1 and 3.2,  $F_{x_{t_1}} = 0$ ,  $p_{2|1} = 1 - p_{1|1}$  and the final model is given by:

$$F_Y = p_{1|1}F_{Y|(1,1)} + (1 - p_{1|1})F_{Y|(1,2)}. \quad (30)$$

If Equations (16) and (18) are considered, then cdf (30) depends on 7 parameters. As an example, let probability  $p_{1|1}$  be equal to 0.15,  $a_{Y|(1,1)}$  be equal to 20,  $b_{Y|(1,1)}$  be equal to  $-1$  and  $\sigma_{Y|(1,1)}$  be equal to 0.3,  $a_{Y|(1,2)}$  be equal to 35,  $b_{Y|(1,2)}$  be equal to  $-1.5$  and  $\sigma_{Y|(1,2)}$  be equal to 0.6, then model (30) becomes:

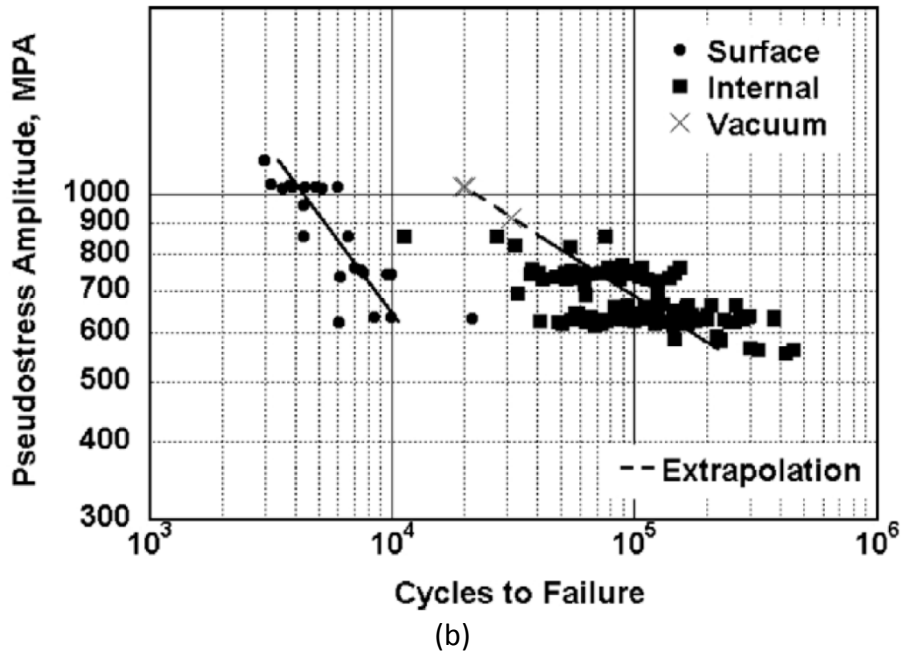
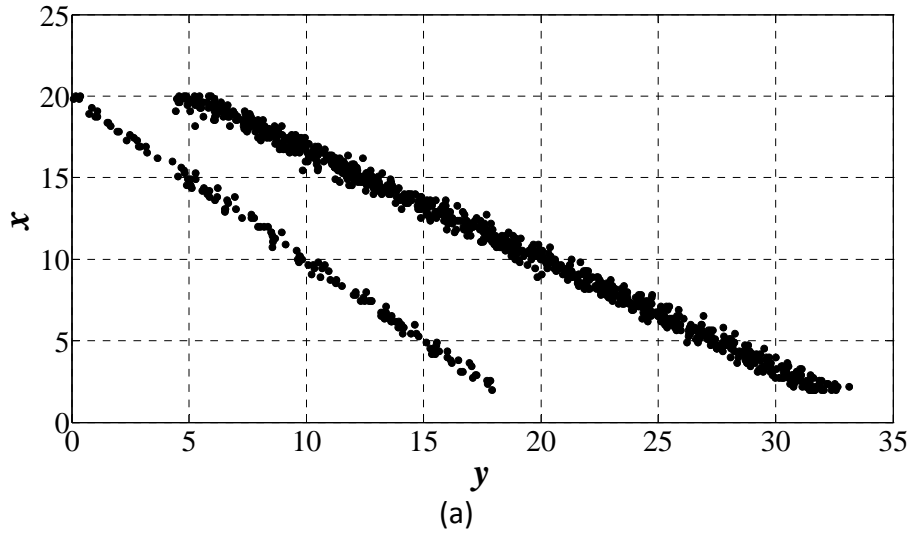
$$F_Y = 0.15 \cdot \Phi\left(\frac{y-(20-x)}{0.3}\right) + 0.85 \cdot \Phi\left(\frac{y-(35-1.5x)}{0.6}\right). \quad (31)$$

Figure 17a shows the S-N curves obtained by using model (31) with failure probabilities equal to 0.1, 0.5 and 0.9, respectively. As shown in Figure 17b, the cdf's at three different  $x$  have the typical shape of a mixture of distributions but they differ in the plateau lengths. In particular, plateau length increases if the applied stress amplitude decreases.



**Figure 17:** (a) S-N curves calculated from model (31) for different failure probabilities. (b) Cdf's of  $Y$  for different values of  $x$ .

Figure 18 shows the good qualitative agreement between random data (Figure 18a) generated by using model (31) and experimental data (Figure 18b) obtained, e.g., on René 95 nickel-base superalloy specimens<sup>11</sup>.



**Figure 18:** (a) Random generated data from model (31). (b) Experimental fatigue data plot<sup>11</sup>.

Random data are generated by considering 100 equispaced values of  $x$  varying from 2 to 20. For each value of  $x$ , 10 random fatigue life values are generated with the procedure explained in Section 4.1.

#### 4.8 One failure mode due to two causes with fatigue limit

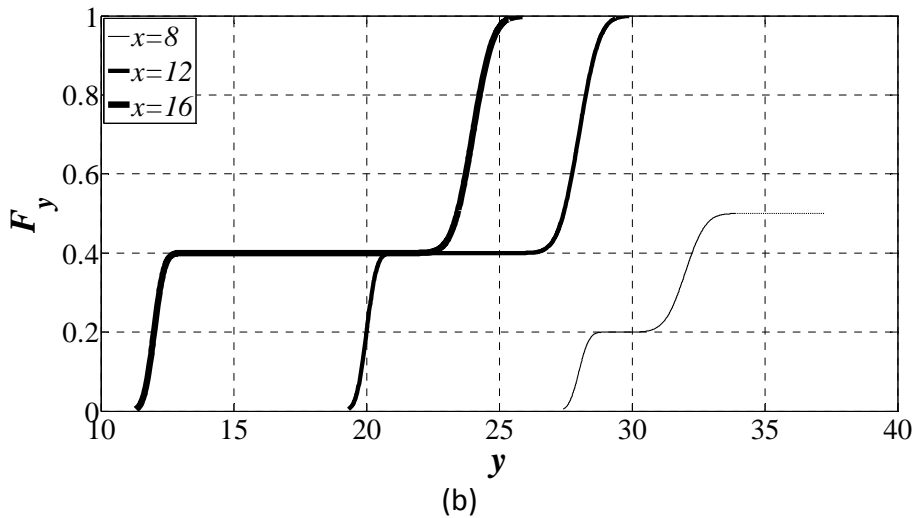
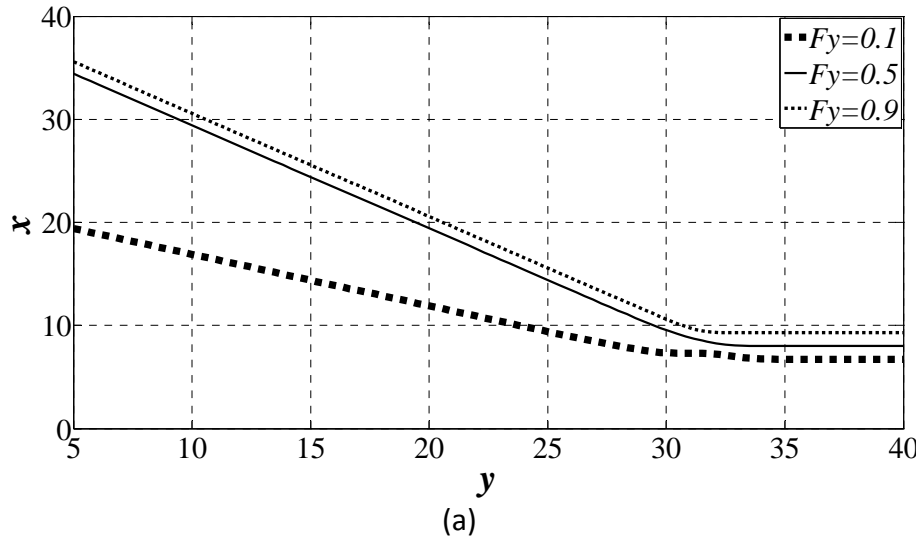
In this case,  $m = 1$ ,  $c_1 = 2$  and  $F_{X_l} = 1$ . According to what stated in Sections 3.1 and 3.2,  $F_{X_{t_1}} = 0$ ,  $p_{2|1} = 1 - p_{1|1}$  and the final model is given by:

$$F_Y = F_{X_l}(p_{1|1}F_{Y|(1,1)} + (1 - p_{1|1})F_{Y|(1,2)}). \quad (32)$$

If Equations (16) and (18) are considered, then cdf (32) depends on 9 parameters. As an example, let probability  $p_{1|1}$  be equal to 0.4,  $a_{Y|(1,1)}$  be equal to 44,  $b_{Y|(1,1)}$  be equal to  $-2$ ,  $\sigma_{Y|(1,1)}$  be equal to 0.3,  $a_{Y|(1,2)}$  be equal to 40,  $b_{Y|(1,2)}$  be equal to  $-1$ ,  $\sigma_{Y|(1,2)}$  be equal to 0.6,  $\mu_{X_l}$  be equal to 8,  $\sigma_{X_l}$  be equal to 1, then model (32) becomes:

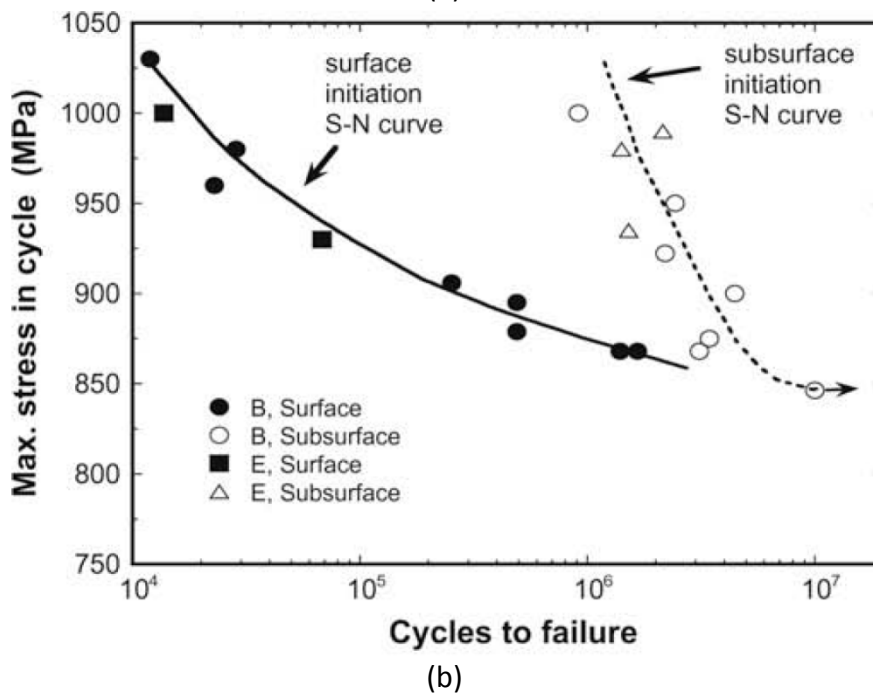
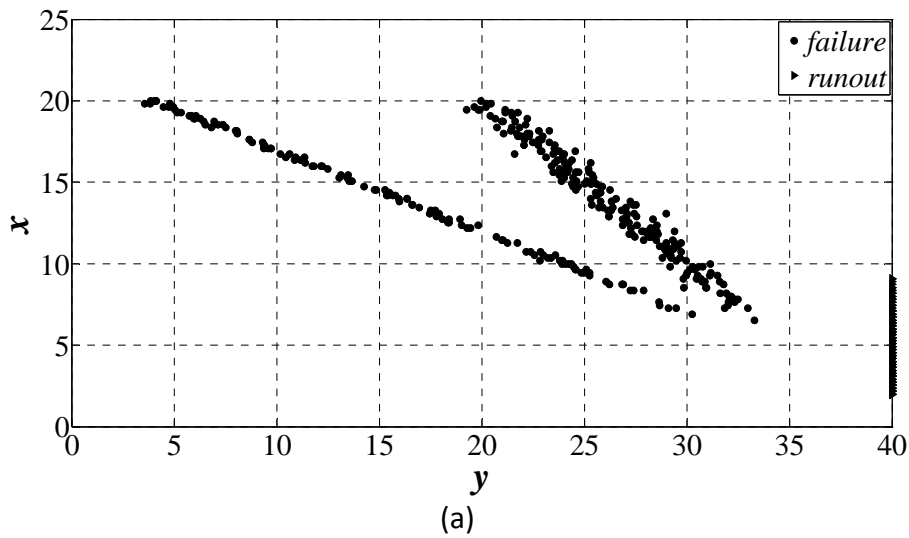
$$F_Y = \Phi(x - 8) \left( 0.4 \cdot \Phi\left(\frac{y - (44 - 2x)}{0.3}\right) + 0.6 \cdot \Phi\left(\frac{y - (40 - x)}{0.6}\right) \right). \quad (33)$$

Figure 19a shows the S-N curves obtained by using model (33) with failure probabilities equal to 0.1, 0.5 and 0.9, respectively. As shown in Figure 19b, the cdf's at three different  $x$  values have the typical shape of a mixture of distributions. Nevertheless, if the applied stress amplitude approaches the fatigue limit, the shape of the cdf's change. In particular, the cdf corresponding to  $x = 8$  gives infinite number of cycles to failure for values of  $F_Y$  larger than  $\Phi_N(8 - 8) = 0.5$ .



**Figure 19:** (a) S-N curves calculated from model (33) for different failure probabilities. (b) Cdf's of  $Y$  for different values of  $x$ .

Figure 20 shows the acceptable qualitative agreement between random data (Figure 20a) generated by using model (33) and experimental data (Figure 20b) obtained, e.g., on Ti-10V-2Fe-3Al  $\beta$ -titanium alloy specimens<sup>11</sup>. It is worth noting that, in this particular case, a quadratic dependence between the location parameter and the stress amplitude would have given random data better resembling the experimental data trends. Nevertheless, a linear dependence has been still considered for sake of simplicity and for coherency with the previous numerical examples.



**Figure 20:** (a) Random generated data from model (33). (b) Experimental fatigue data plot<sup>11</sup>; different curves correspond to different microstructures.

Random data are generated by considering 100 equispaced values of  $x$  varying from 2 to 20. For each value of  $x$ , 5 random fatigue life values are generated with the procedure explained in Section 4.2.

## 5. Conclusions

A unified statistical model able to describe any S-N curve regardless of the number of failure modes and failure causes has been identified. Assuming that the random variables involved in the model follow location-scale distributions, that the location parameters linearly depend on the applied stress amplitude and the scale parameters are constant, a general equation for the total number of parameters to be estimated is obtained.

The proposed model allows to fit experimental data with any number of failure modes and failure causes. A full probabilistic approach is adopted to obtain the distribution of the fatigue life.

Different causes for each failure mode and different failure modes are taken into account by considering an approach based on a mixture of distributions. The adaptability of the model is demonstrated by qualitative numerical examples.

## References

- 1 Pyttel, B., Schwerdt, D. and Berger, C. (2011) Very high cycle fatigue – Is there a fatigue limit? *Int. J. Fatigue* **33**, 49-58.
- 2 Shiozawa, K., Lu, L. and Ishihara, S. (2001) S-N curve characteristics and subsurface crack initiation behaviour in ultra-long life of fatigue of a high carbon-chromium bearing steel. *Fatigue Fract. Engng. Mater. Struct.* **24**, 781-790.
- 3 Wang, Q.Y., Bathias, C., Kawagoishi, N. and Chen, Q. (2002) Effect of inclusions on subsurface crack initiation and gigacycle fatigue strength. *Int. J. Fatigue* **24**, 1269-1274.
- 4 Sakai, T., Sakai, T., Okada, K., Furuichi, M., Nishikawa, I. and Sugeta, A. (2006) Statistical fatigue properties of SCM435 steel in ultra-long-life regime based on JSMS database on fatigue strength of metallic materials. *Int. J. Fatigue* **28**, 1486-1492.
- 5 Zhang, J.M., Li, S.X., Yang, Z.G., Li, G.Y., Hui, W.J. and Weng Y.Q. (2007) Influence of inclusion size on fatigue behavior of high strength steels in the gigacycle fatigue regime. *Int. J. Fatigue* **29**, 765-771.
- 6 Sakai, T., Lian, B., Takeda, M., Shiozawa, K., Oguma, N., Ochi, Y., Nakajima, M. and Nakamura, T. (2010) Statistical duplex S-N characteristics of high carbon chromium bearing steel in rotating bending in very high cycle regime. *Int. J. Fatigue* **32**, 497-504.
- 7 Bathias, C. (1999) There is no infinite fatigue life in metallic materials. *Fatigue Fract. Engng. Mater. Struct.* **22**, 559-565.
- 8 Jha, S.K., Larsen, J.M. and Rosenberger, A.H. (2005) The role of competing mechanisms in the fatigue life variability of a nearly fully-lamellar  $\gamma$ -TiAl based alloy. *Acta Mater.* **53**, 1293-1304.
- 9 Ravi Chandran, K.S. (2005) Duality of fatigue failures of materials caused by Poisson defect statistics of competing failure modes. *Nat. Mater.* **4**, 303-308.
- 10 Furuya, Y., Hirukawa, H., Kimura, T. and Hayaishi, M. (2007) Gigacycle fatigue properties of high-strength steels according to inclusion and ODA Sizes. *Metall. Mater. Trans. A-Phys. Metall. Mater. Sci.* **38A**, 1722-1730.
- 11 Ravi Chandran, K.S., Chang, P. and Cashman, G.T. (2010) Competing failure modes and complex S-N curves in fatigue of structural materials. *Int. J. Fatigue* **32**, 482-491.
- 12 Cashman, G.T. (2010) A review of competing modes fatigue behavior. *Int. J. Fatigue* **32**, 492-496.
- 13 Murakami, Y. (2002) *Metal Fatigue: Effect of Small Defects and Nonmetallic Inclusions*. Elsevier, Oxford, UK.
- 14 Harlow, D.G. (2011) Statistical characterization of bimodal behavior. *Acta Mater.*, **59**, 5048-5053.



- 15 ASTM E739-91 Reapproved 2004 (2004) *Standard Practice for Statistical Analysis of Linear or Linearized Stress-Life (S-N) and Strain-Life ( $\epsilon$ -N) Fatigue Data*. ASTM, Philadelphia, USA.
- 16 ISO standard 12107:2003 (2003) *Metallic materials – Fatigue testing – Statistical planning and analysis of data*. ISO, Genève, Switzerland.
- 17 Pascual, F.G. and Meeker, W.Q. (1999) Estimating fatigue curves with the Random Fatigue-Limit Model. *Technometrics* **41**, 277-290.
- 18 Lorén, S. and Lundström, M. (2005) Modelling curved S-N curves. *Fatigue Fract. Engng. Mater. Struct.* **28**, 437-443.
- 19 Castillo, E. and Fernández-Canteli, A. (2001) A general regression model for lifetime evaluation and prediction. *Int. J. Fract.* **107**, 117-137.
- 20 Hanaki, S., Yamashita, M., Uchida, H. and Zako, M. (2010) On stochastic evaluation of S-N data based on fatigue strength distribution. *Int. J. Fatigue* **32**, 605-609.
- 21 Cashman, G.T. (2007) A statistical methodology for the preparation of a competing modes fatigue design curve. *J. Engng. Mater. Technol.* **129**, 159-168.
- 22 Cashman, G.T. (2007) A mathematical model for competing failure modes in strain cycle fatigue. *J. Engng. Mater. Technol.* **129**, 293-303.
- 23 Bomas, H., Burkart, K. and Zoch, H.W. (2011) Evaluation of S-N curves with more than one failure mode. *Int. J. Fatigue* **33**, 19-22.
- 24 Cox, D.R. (1959) The analysis of exponentially distributed life-times with two types of failure. *J. R. Stat. Soc. Ser. B-Stat. Methodol.* **21**, 411-421.
- 25 Nelson, W. (1982) *Applied Life Data Analysis*. John Wiley & Sons, New York, USA, pp. 162-168.
- 26 Jha, S.K., Larsen, J.M., Rosenberger, A.H. and Hartman, G.A. (2003) Dual fatigue failure modes in Ti-6Al-2Sn-4Zr-6Mo and consequences on probabilistic life prediction. *Scr. Mater.* **48**, 1637-1642.
- 27 Mendenhall, W. and Hader, R.J. (1958) Estimation of parameters of mixed exponentially distributed failure time distributions from censored life test data. *Biometrika* **45**, 504-520.
- 28 Ravi Chandran, K.S. and Jha, S.K. (2005) Duality of the S-N fatigue curve caused by competing failure modes in titanium alloy and the role of Poisson defect statistics. *Acta Mater.* **53**, 1867-1881.
- 29 Nelson, W. (1990) *Accelerated Testing: Statistical Models, Test Plans, and Data Analyses*. John Wiley & Sons, New York, USA, pp. 71-75.
- 30 Nelson, W. (1990) *Accelerated Testing: Statistical Models, Test Plans, and Data Analyses*. John Wiley & Sons, New York, USA, pp. 92-95.

31 Marines, I., Bin, X. and Bathias, C. (2003) An understanding of very high cycle fatigue of metals. *Int. J. Fatigue* **25**, 1101-1107.

32 NRIM Fatigue Data Sheet No. 6 (1974), *Data sheets on elevated-temperature, high-cycle fatigue properties of SUS 403-B (12Cr) stainless steel bar for turbine blades*. National Research Institute for Metals, Tokyo, Japan.

33 Berger, C. and Kaiser, B. (2006) Results of very high cycle fatigue tests on helical compression springs. *Int. J. Fatigue* **28**, 1658-1663.

34 NIMS Fatigue Data Sheet No. 98 (2005), *Data sheet on giga-cycle fatigue properties of Ti-6Al-4V (1100 MPa class) titanium alloy*. National Institute for Materials Science, Tokyo, Japan.